

Chiral effective field theory for nuclear forces

Summary day 4

- Pion exchange has to be treated non-perturbatively \Rightarrow finite-cutoff formulation of chiral EFT
- Nuclear forces and currents = non-iterative contributions to the amplitude. They obey the standard ChPT power counting and can be derived e.g. using the MUT

Today: State-of-the-art and applications

Outline Day 5

1. The 2N system

- regularization, determination of LECs, uncertainty quantification, ...
- precision determination of the pion-nucleon coupling constants

2. The 3N-force challenge

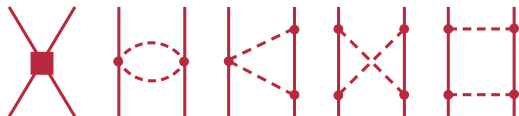
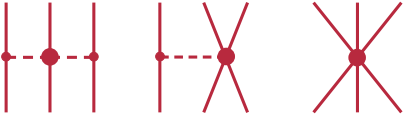
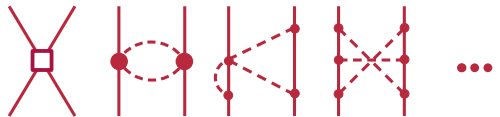
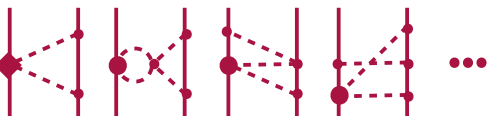
3. Electroweak currents

4. Chiral EFT and lattice QCD

5. Nuclear lattice simulations

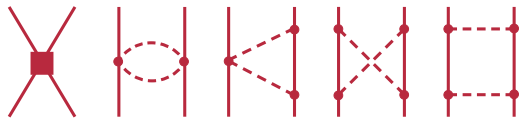
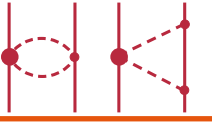
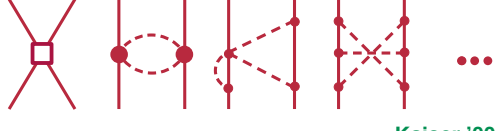
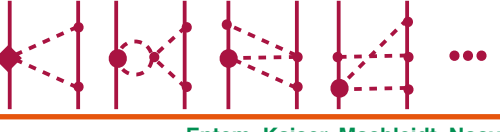
6. Summary Day 5

Nuclear Hamiltonian: State-of-the-art [W-counting]

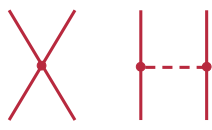
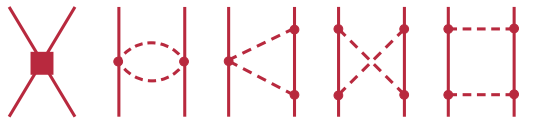
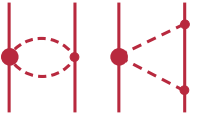
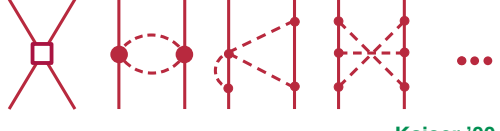
	Two-nucleon force	Three-nucleon force	Four-nucleon force
LO (Q^0)			
	Weinberg '90		
NLO (Q^2)			
	Ordonez, van Kolck '92		
N ² LO (Q^3)			
	Ordonez, van Kolck '92	van Kolck '94; EE et al. '02	
N ³ LO (Q^4)			
	Kaiser '00 - '02	Bernard, EE, Krebs, Meißner, '08, '11	EE '06
N ⁴ LO (Q^5)			
	Entem, Kaiser, Machleidt, Nosyk '15 EE, Krebs, Meißner '15	Girlanda, Kievsky, Viviani '11 Krebs, Gasparyan, EE '12, '13 (short-range loop contrib. still missing)	(preliminary)

Chiral power counting provides a natural explanation for the observed hierarchy of nuclear forces!
 Similar program is being carried out in chiral EFT with $\Delta(1232)$ [Ordonez et al., Kaiser et al., Krebs, EE, Meißner].

Nuclear Hamiltonian: State-of-the-art [W-counting]

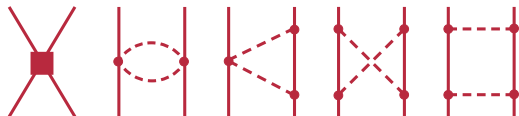
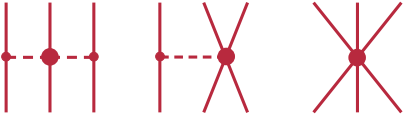
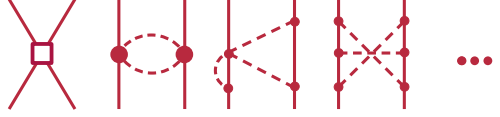
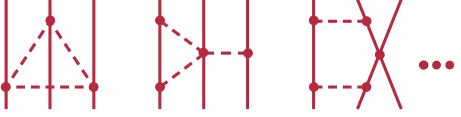
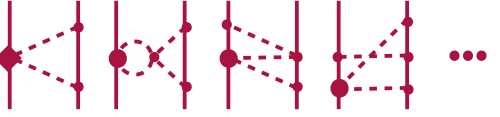
	Two-nucleon force	Three-nucleon force	Four-nucleon force
LO (Q^0)			
	Weinberg '90		
NLO (Q^2)			
	Ordonez, van Kolck '92		
N ² LO (Q^3)	<div style="border: 2px solid orange; padding: 5px; display: inline-block;">  <p style="margin: 0;">parameter-free: πN LECs from Roy-Steiner</p> </div>		
	Ordonez, van Kolck '92	van Kolck '94; EE et al. '02	
N ³ LO (Q^4)		<div style="border: 2px solid orange; padding: 5px; display: inline-block;">  </div>	<div style="border: 2px solid orange; padding: 5px; display: inline-block;">  </div>
	Kaiser '00 - '02	Bernard, EE, Krebs, Meißner, '08, '11	EE '06
N ⁴ LO (Q^5)	<div style="border: 2px solid orange; padding: 5px; display: inline-block;">  </div>		 <p>(preliminary)</p>
	Entem, Kaiser, Machleidt, Nosyk '15 EE, Krebs, Meißner '15	Girlanda, Kievsky, Viviani '11 Krebs, Gasparyan, EE '12, '13 (short-range loop contrib. still missing)	

Nuclear Hamiltonian: State-of-the-art [W-counting]

	Two-nucleon force	Three-nucleon force	Four-nucleon force
LO (Q^0)			
	Weinberg '90		
NLO (Q^2)			
	Ordonez, van Kolck '92		
N ² LO (Q^3)			
	Ordonez, van Kolck '92	van Kolck '94; EE et al. '02	
N ³ LO (Q^4)			
	Kaiser '00 - '02	Bernard, EE, Krebs, Meißner, '08, '11	EE '06
N ⁴ LO (Q^5)			
	Entem, Kaiser, Machleidt, Nosyk '15 EE, Krebs, Meißner '15	Girlanda, Kievsky, Viviani '11 Krebs, Gasparyan, EE '12, '13 (short-range loop contrib. still missing)	(preliminary)

Scheme dependence (unitary ambiguity) starts showing up at N³LO: **2 phases** ($\bar{\beta}_8$, $\bar{\beta}_9$) in the long-range relativistic corrections + **3 off-shell short-range terms** in the 1S_0 , 3S_1 and ε_1 channels.

Nuclear Hamiltonian: State-of-the-art [W-counting]

	Two-nucleon force	Three-nucleon force	Four-nucleon force
LO (Q^0)			
	Weinberg '90		
NLO (Q^2)			
	Ordonez, van Kolck '92		
N ² LO (Q^3)			
	Ordonez, van Kolck '92	van Kolck '94; EE et al. '02	
N ³ LO (Q^4)			
	Kaiser '00 - '02	Bernard, EE, Krebs, Meißner, '08, '11	EE '06
N ⁴ LO (Q^5)			
	Entem, Kaiser, Machleidt, Nosyk '15 EE, Krebs, Meißner '15	Girlanda, Kievsky, Viviani '11 Krebs, Gasparyan, EE '12, '13 (short-range loop contrib. still missing)	(preliminary)

The published expressions for the nuclear forces make use of dimensional regularization for loop integrals. **Additional regularization is required when solving the Schrödinger equation!**

The 2N system

The NN potential from chiral EFT

P. Reinert, H. Krebs, EE, EPJA 54 (2018) 88

So far, discussed the derivation of chiral potentials (using DR). Next steps:

- determination of the πN LECs to fix the long-range nuclear force
- regularization
- determination of the contact interactions (implicit renormalization)

1. Determination of πN LECs

Effective chiral Lagrangian:

$$\mathcal{L}_\pi = \mathcal{L}_\pi^{(2)} + \mathcal{L}_\pi^{(4)} + \dots$$

$$\mathcal{L}_{\pi N} = \underbrace{\bar{N} \left(i\gamma^\mu D_\mu[\pi] - m + \frac{g_A}{2} \gamma^\mu \gamma_5 u_\mu[\pi] \right) N}_{\mathcal{L}_{\pi N}^{(1)}} + \underbrace{\sum_i \mathbf{c}_i \bar{N} \hat{O}_i^{(2)}[\pi] N}_{\mathcal{L}_{\pi N}^{(2)}} + \underbrace{\sum_i \mathbf{d}_i \bar{N} \hat{O}_i^{(3)}[\pi] N}_{\mathcal{L}_{\pi N}^{(3)}} + \underbrace{\sum_i \mathbf{e}_i \bar{N} \hat{O}_i^{(4)}[\pi] N}_{\mathcal{L}_{\pi N}^{(4)}} + \dots$$

low-energy constants

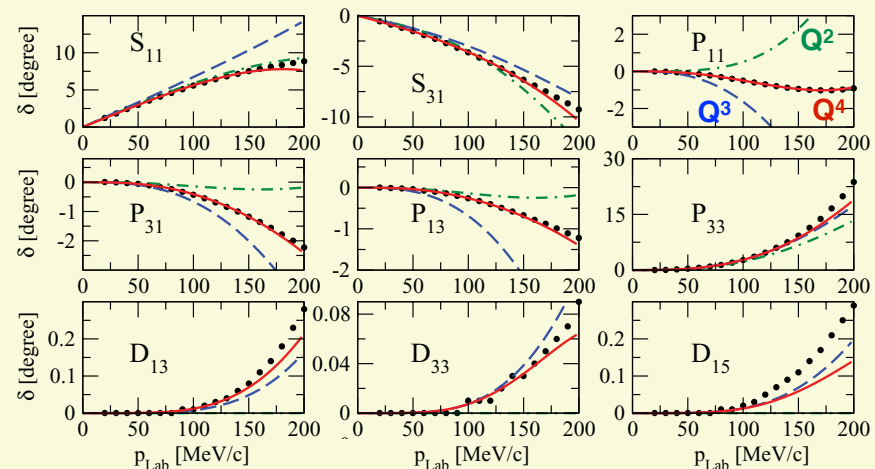
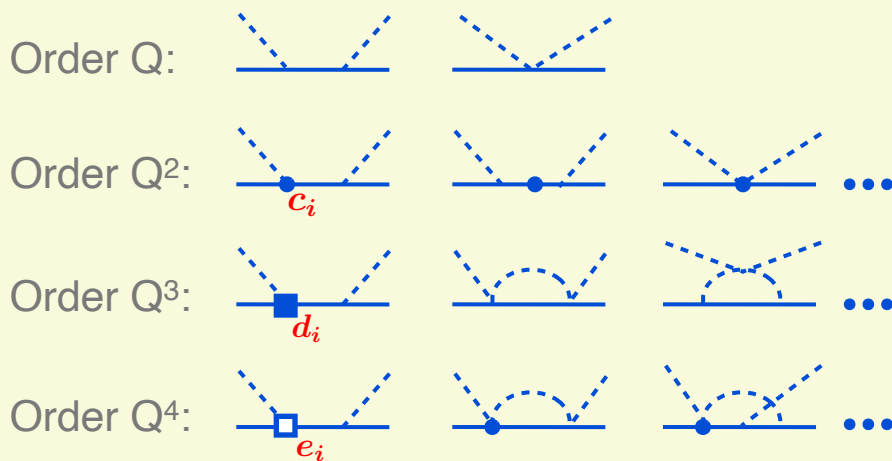
Pion-nucleon scattering amplitude for $\pi^a(q_1) + N(p_1) \rightarrow \pi^b(q_2) + N(p_2)$:

$$T_{\pi N}^{ba} = \frac{E + m}{2m} \left(\delta^{ba} \left[g^+(\omega, t) + i\vec{\sigma} \cdot \vec{q}_2 \times \vec{q}_1 h^+(\omega, t) \right] + i\epsilon^{bac} \tau^c \left[g^-(\omega, t) + i\vec{\sigma} \cdot \vec{q}_2 \times \vec{q}_1 h^-(\omega, t) \right] \right)$$

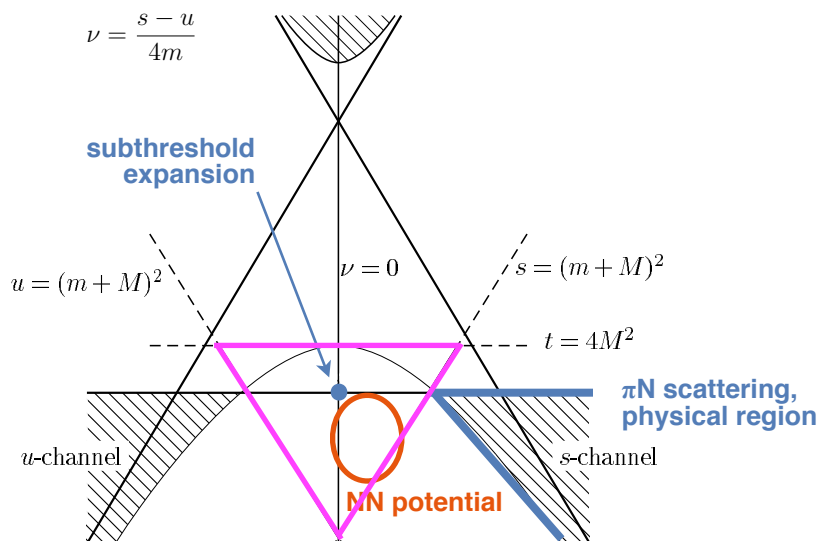
calculated within the chiral expansion

Pion-nucleon scattering up to Q^4 in heavy-baryon ChPT

Fettes, Meißner '00; Krebs, Gasparyan, EE '12



1. Determination of πN LECs



Matching ChPT to πN Roy-Steiner equations

Hoferichter, Ruiz de Elvira, Kubis, Meißner, PRL 115 (2015) 092301

- χ expansion of the πN amplitude expected to converge best within the Mandelstam triangle
- Subthreshold coefficients (from RS analysis) provide a natural matching point to ChPT

$$\bar{X} = \sum_{m,n} x_{mn} \nu^{2m+k} t^n, \quad X = \{A^\pm, B^\pm\}$$

- Closer to the kinematics relevant for nuclear forces...

Relevant LECs (in GeV^{-n}) extracted from πN scattering

	c_1	c_2	c_3	c_4	$\bar{d}_1 + \bar{d}_2$	\bar{d}_3	\bar{d}_5	$\bar{d}_{14} - \bar{d}_{15}$	\bar{e}_{14}	\bar{e}_{17}	
$[Q^4]_{\text{HB, NN, GW PWA}}$	-1.13	3.69	-5.51	3.71	5.57	-5.35	0.02	-10.26	1.75	-0.58	} Krebs, Gasparyan, EE, PRC85 (12) 054006
$[Q^4]_{\text{HB, NN, KH PWA}}$	-0.75	3.49	-4.77	3.34	6.21	-6.83	0.78	-12.02	1.52	-0.37	
$[Q^4]_{\text{HB, NN, Roy-Steiner}}$	-1.10	3.57	-5.54	4.17	6.18	-8.91	0.86	-12.18	1.18	-0.18	} Hoferichter et al., PRL 115 (15) 092301
$[Q^4]_{\text{covariant, data}}$	-0.82	3.56	-4.59	3.44	5.43	-4.58	-0.40	-9.94	-0.63	-0.90	} Siemens et al., PRC94 (16) 014620

– Some LECs show sizable correlations (especially c_1 and c_3)...

– RKE N⁴LO [Reinert, Krebs, EE, EPJA 54 (2018) 88]: **Q⁴ fit to RS** and **Q⁴ fit to KH PWA**

With the LECs taken from πN , the long-range NN force is completely fixed (parameter-free)

2. Regularization

The cutoff Λ has to be kept finite, $\Lambda \sim \Lambda_b$ (unless all counterterms are taken into account in the calculations) [Lepage '97; EE, Gegelia '09]. In practice, low values of Λ are preferred:

- many-body methods require soft interactions,
- spurious deeply-bound states for $\Lambda > \Lambda^{\text{crit}}$ make calculations for $\Lambda > 3$ unfeasible...

→ it is crucial to employ a regulator that minimizes finite- Λ artifacts!

Nonlocal: $V_{1\pi}^{\text{reg}} \propto \frac{e^{-\frac{p'^4+p^4}{\Lambda^4}}}{\vec{q}^2 + M_\pi^2} \longrightarrow \frac{1}{\vec{q}^2 + M_\pi^2} \underbrace{\left(1 - \frac{p'^4 + p^4}{\Lambda^4} + \mathcal{O}(\Lambda^{-8})\right)}_{\text{affect long-range interactions...}}$

EE, Glöckle, Meißner '04;
Entem, Machleidt '03;
Entem, Machleidt, Nosyk '17; ...

Local: $V_{1\pi}^{\text{reg}} \propto \frac{e^{-\frac{\vec{q}^2 + M_\pi^2}{\Lambda^2}}}{\vec{q}^2 + M_\pi^2} \longrightarrow \frac{1}{\vec{q}^2 + M_\pi^2} \left(1 + \text{short-range terms}\right)$

[inspired by Thomas Rijken] Reinert, Krebs, EE '18;

→ does not affect long-range physics at any order in $1/\Lambda^2$ -expansion

- Application to 2π exchange does not require re-calculating the corresponding diagrams:

$$V(q) = \frac{2}{\pi} \int_{2M_\pi}^{\infty} \mu d\mu \frac{\rho(\mu)}{q^2 + \mu^2} + \dots \xrightarrow{\text{reg.}} V_\Lambda(q) = e^{-\frac{q^2}{2\Lambda^2}} \frac{2}{\pi} \int_{2M_\pi}^{\infty} \mu d\mu \frac{\rho(\mu)}{q^2 + \mu^2} e^{-\frac{\mu^2}{2\Lambda^2}} + \dots$$

polynomial in q^2, M_π

- Convention: choose polynomial terms such that $\Delta^n V_{\Lambda, \text{long}}(\vec{r})|_{r=0} = 0$

2. Regularization

The general structure of the long-range potential is:

$$V(\vec{q}, \vec{k}) = V_C(q) + \boldsymbol{\tau}_1 \cdot \boldsymbol{\tau}_2 W_C(q) + [V_S(q) + \boldsymbol{\tau}_1 \cdot \boldsymbol{\tau}_2 W_S(q)] \vec{\sigma}_1 \cdot \vec{\sigma}_2 + [V_T(q) + \boldsymbol{\tau}_1 \cdot \boldsymbol{\tau}_2 W_T(q)] \vec{\sigma}_1 \cdot \vec{q} \vec{\sigma}_2 \cdot \vec{q} \\ + [V_{LS}(q) + \boldsymbol{\tau}_1 \cdot \boldsymbol{\tau}_2 W_{LS}(q)] i(\vec{\sigma}_1 + \vec{\sigma}_2) \cdot (\vec{q} \times \vec{k})$$

Consider the NLO TPEP $W_C(q)$ as an example:

$$W_C^{(2)}(q) = -\frac{1}{384\pi^2 F_\pi^4} \left[4M_\pi^2(5g_A^4 - 4g_A^2 - 1) + q^2(23g_A^4 - 10g_A^2 - 1) + \frac{48g_A^4 M_\pi^4}{4M_\pi^2 + q^2} \right] L(q)$$

$$\frac{\sqrt{q^2 + 4M_\pi^2}}{q} \ln \frac{\sqrt{q^2 + 4M_\pi^2} + q}{2M_\pi}$$

Dispersive representation: $W_C^{(2)}(q) = \frac{2}{\pi} \int_{2M_\pi}^{\infty} \frac{d\mu}{\mu^3} q^4 \frac{\rho(\mu)}{\mu^2 + q^2} + \alpha + \beta q^2$ with $\rho(\mu) = \text{Im} [W_C^{(2)}(0^+ - i\mu)]$

(Notice: $\text{Im} [L(0^+ - i\mu)] = \sqrt{\mu^2 - 4M_\pi^2}/\mu$).

Regularization and subtractions:

$$W_{C,\Lambda}^{(2)}(q) = \frac{2}{\pi} \int_{2M_\pi}^{\infty} \frac{d\mu}{\mu^3} \rho(\mu) \left(\frac{q^4}{\mu^2 + q^2} + \underbrace{C_{C,1}^2(\mu) + C_{C,2}^2(\mu) q^2}_{\text{chosen to enforce: } W_{C,\Lambda}^{(2)}(r)|_{r=0} = \frac{d^2}{dr^2} W_{C,\Lambda}^{(2)}(r)|_{r=0} = 0} \right) e^{-\frac{\mu^2 + q^2}{2\Lambda^2}}$$

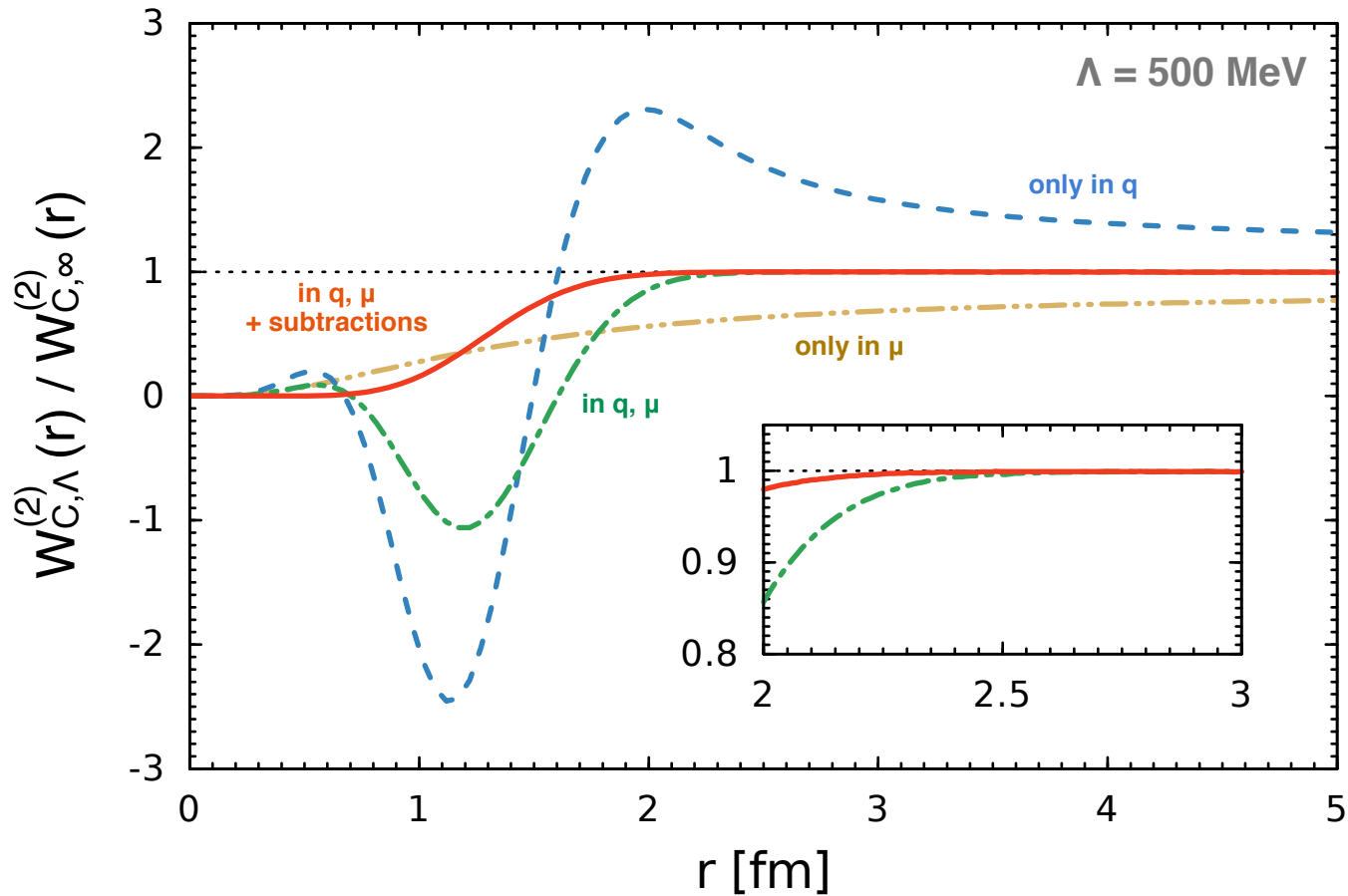
$$\text{chosen to enforce: } W_{C,\Lambda}^{(2)}(r)|_{r=0} = \frac{d^2}{dr^2} W_{C,\Lambda}^{(2)}(r)|_{r=0} = 0$$

E.g.: $C_{C,1}^2(\mu) = \frac{2\Lambda\mu^2(2\Lambda^4 - 4\Lambda^2\mu^2 - \mu^4) + \sqrt{2\pi}\mu^5 e^{\frac{\mu^2}{2\Lambda^2}}(5\Lambda^2 + \mu^2) \text{erfc}\left(\frac{\mu}{\sqrt{2}\Lambda}\right)}{4\Lambda^5}$

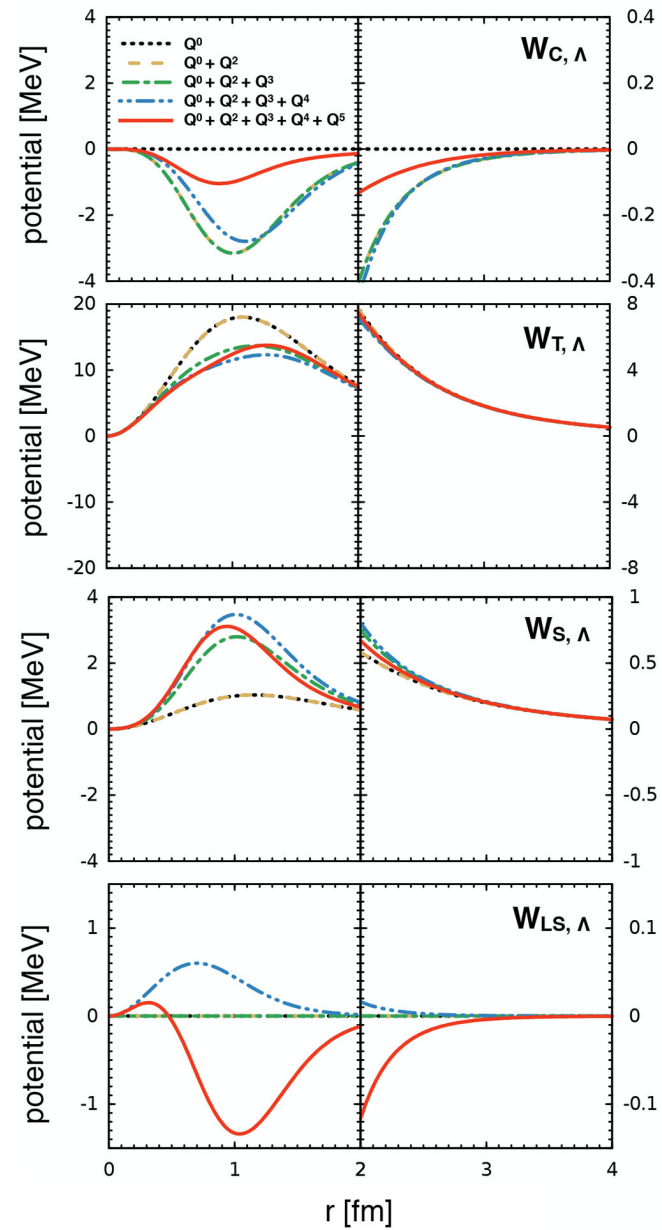
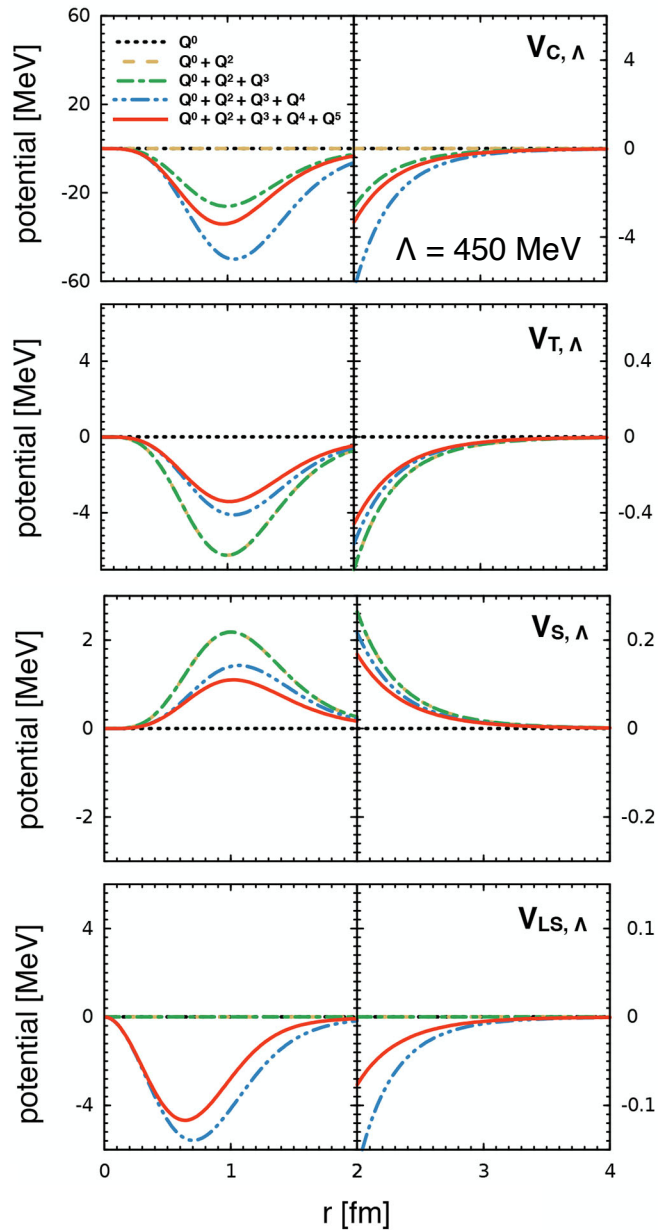
2. Regularization

Regularized 2π -exchange potential:

Various regularization approaches



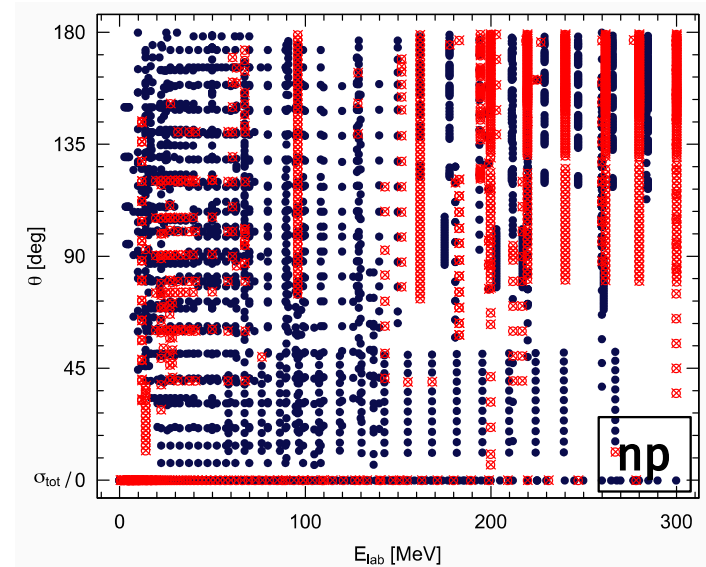
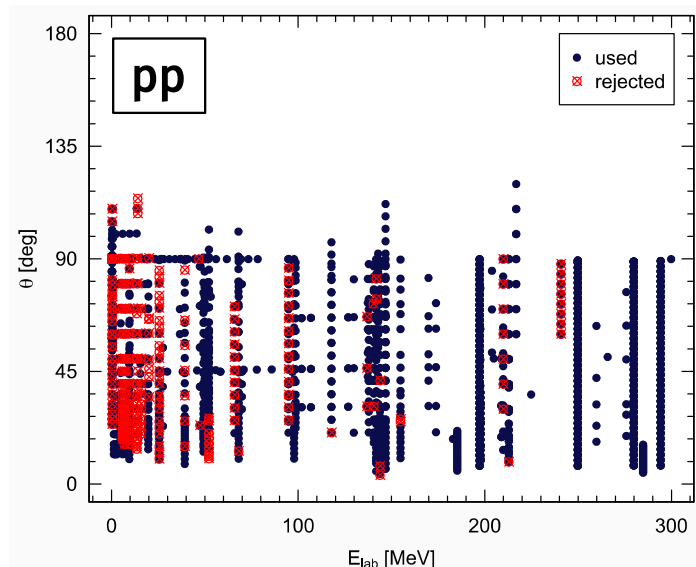
2. Regularization



3. Determination of the NN LECs and results

P. Reinert, H. Krebs, EE, EPJA 54 (2018) 88

- Contacts at N⁴LO⁺: 2 [Q⁰] + 7 [Q²] + **12** [Q⁴] + 4 [F-waves, Q⁶] + IB; Gauss regulator
- Use scattering data together with $B_d = 2.224575(9)$ MeV and $b_{np} = 3.7405(9)$ fm.
- Since 1950-es, about 3000 proton-proton + 5000 neutron-proton scattering data below 350 MeV have been collected.
- However, certain data are mutually incompatible within errors and have to be rejected.
2013 Granada database [Navarro-Perez et al., PRC 88 (2013) 064002], rejection rate: 31% np, 11% pp:
2158 proton-proton + 2697 neutron-proton data below $E_{lab} = 300$ MeV

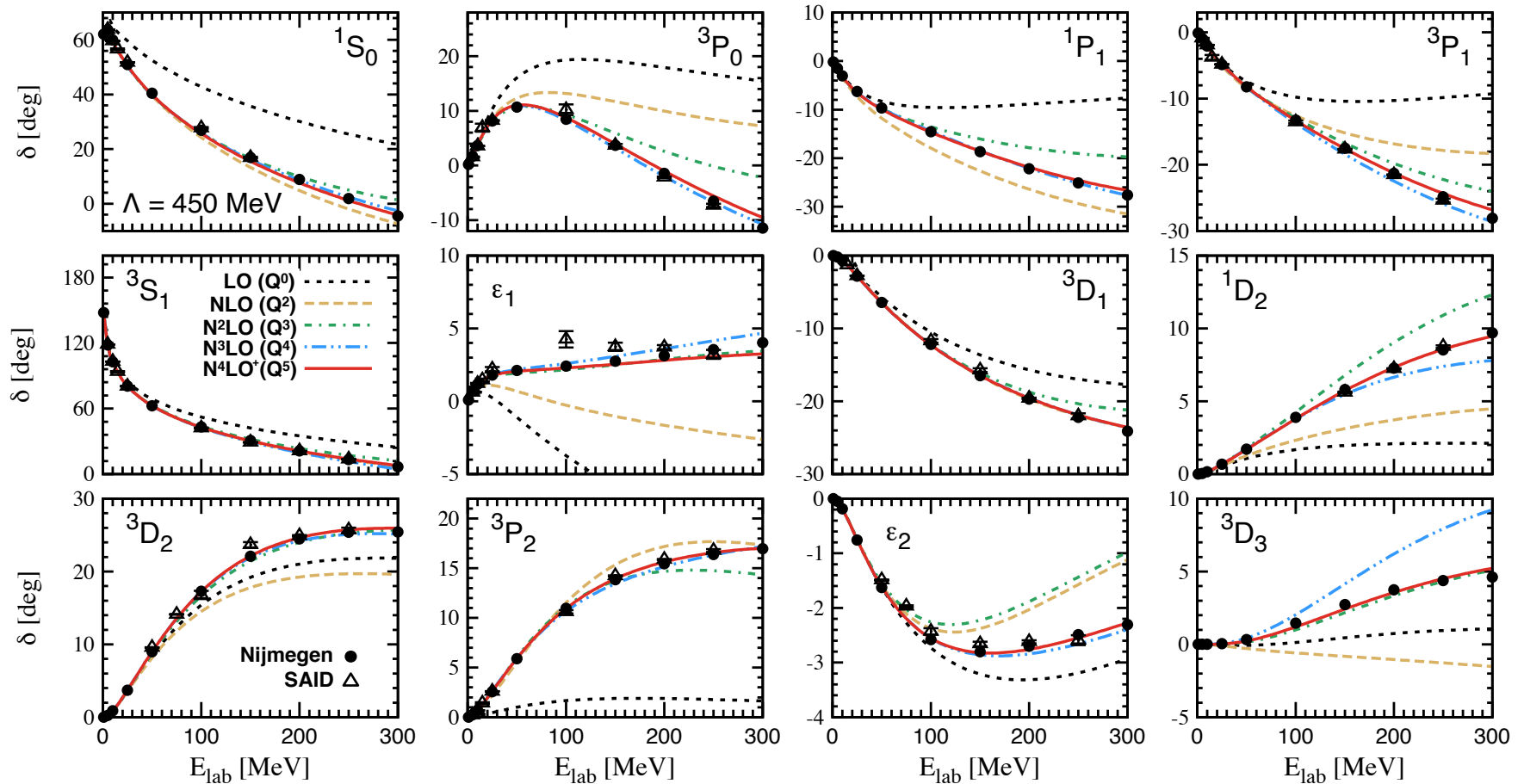


- Incomplete treatment of IB effects: $V_\gamma + V_{1\pi} + V_{cont} ({}^1S_0)$

3. Determination of the NN LECs and results

P. Reinert, H. Krebs, EE, EPJA 54 (2018) 88

Convergence of the chiral expansion for np phase shifts



— Clear evidence of the parameter-free chiral 2π exchange (Roy-Steiner LECs)!

3. Determination of the NN LECs and results

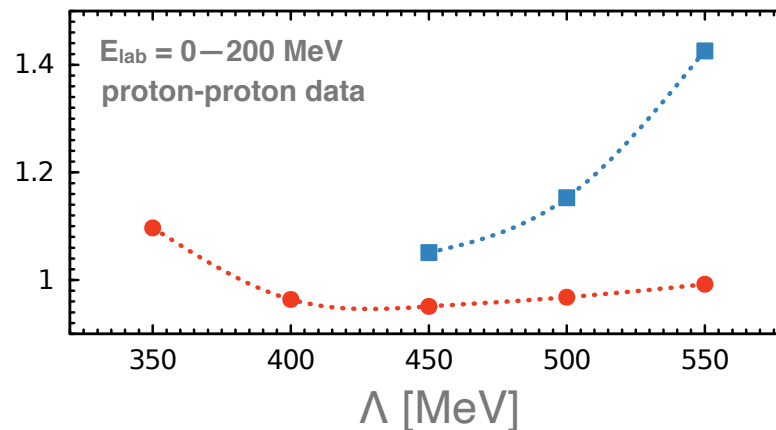
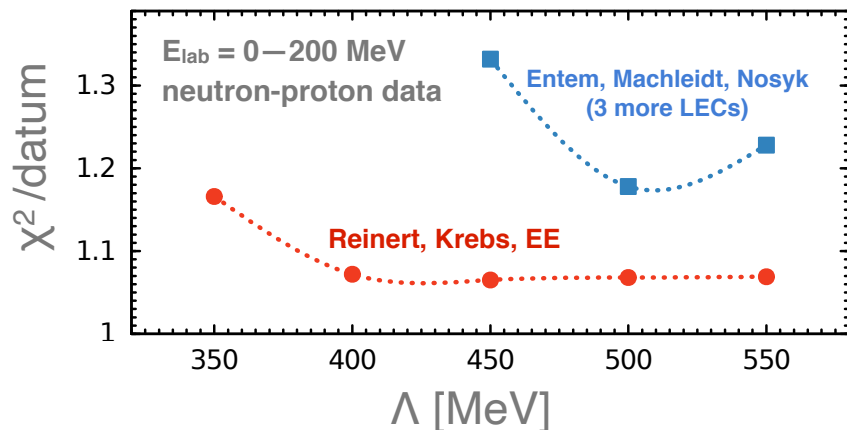
P. Reinert, H. Krebs, EE, EPJA 54 (2018) 88

χ^2 /datum for the description of the Granada-2013 database: χ EFT vs. phenomenology

E_{lab} bin	CD Bonn ₍₄₃₎	Nijm I ₍₄₁₎	Nijm II ₍₄₇₎	Reid93 ₍₅₀₎	$N^4\text{LO}^+$ ₍₂₇₊₁₎ , this work
neutron-proton scattering data					
0 – 100	1.08	1.06	1.07	1.08	1.07
0 – 200	1.08	1.07	1.07	1.09	1.07
0 – 300	1.09	1.09	1.10	1.11	1.06
proton-proton scattering data					
0 – 100	0.88	0.87	0.87	0.85	0.86
0 – 200	0.98	0.99	1.00	0.99	0.95
0 – 300	1.01	1.05	1.06	1.04	1.00

For the first time, chiral EFT potentials qualify for being regarded as PWA!

$N^4\text{LO}^+$: semilocal (Reinert, Krebs, EE) vs. nonlocal (Entem, Machleidt, Nosyk)



4. Truncation uncertainty

In most cases, the uncertainty is dominated by truncation errors. Consider an observable $X(p)$:

$$X(p) = \underbrace{c_0 + c_2 Q^2 + c_3 Q^3 + \dots + c_i Q^i}_{\text{known from explicit calculations}} + \underbrace{c_{i+1} Q^{i+1} + \dots}_{\text{truncation error } \delta X^{(i)} \text{ to be estimated}} \quad \text{where } Q = \max\left(\frac{p}{\Lambda_b}, \frac{M_\pi^{\text{eff}}}{\Lambda_b}\right)$$

Instead of just assuming $c_{i+1} \sim 1$, use the information from the known $c_{0\dots i}$ [EE, Krebs, Meißner '15]

Bayesian approach to estimating truncation errors [Furnstahl et al. (BUQEYE) '15-'21; EE et al. '19]

- assume some common probability distribution function for c_i (= prior pdf)
- calculate the **posterior probability distribution function** $\text{pr}(\delta X^{(i)} | c_{0\dots i})$
- at high chiral orders, almost no dependence on the prior...
- easy to implement and universal

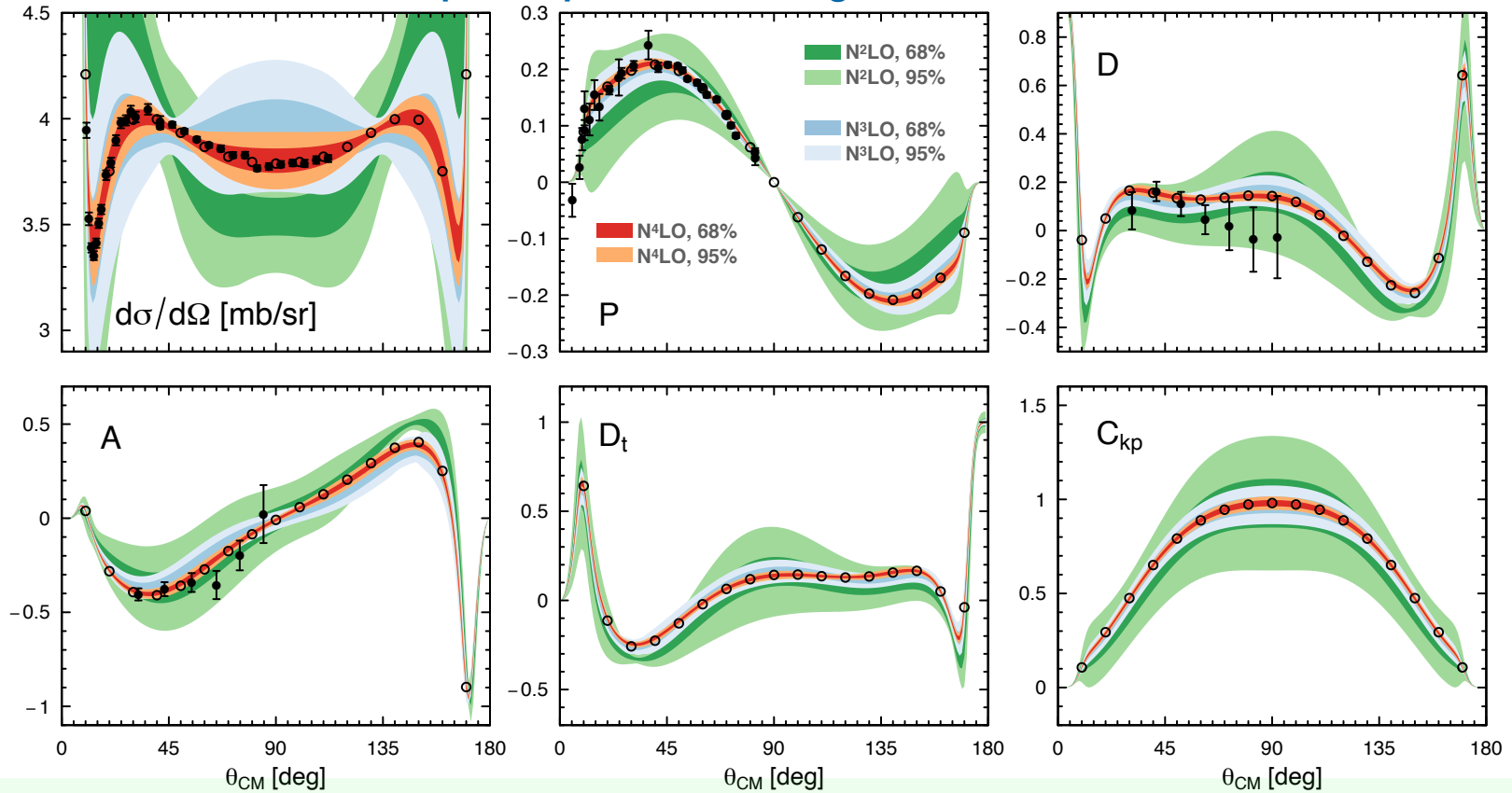
Example: neutron-proton total cross section at 100 MeV [$\Lambda = 450$ MeV]

$$\begin{aligned} \sigma_{\text{tot}} &= 84.0_{[q^0]} - 10.2_{[q^2]} + 0.4_{[q^3]} - 0.4_{[q^4]} + 0.6_{[q^5]} - 0.0_{[q^6]} \\ &= 74.35(14)(17)(1) \text{ mb} \end{aligned}$$

truncation error (68% DoB) \longleftarrow \longleftarrow \longleftarrow uncertainty in the π N LECs
 statistical error (NN LECs) \longleftarrow

4. Truncation uncertainty

Selected proton-proton scattering observables at 143 MeV



Example: neutron-proton total cross section at 100 MeV [$\Lambda = 450$ MeV]

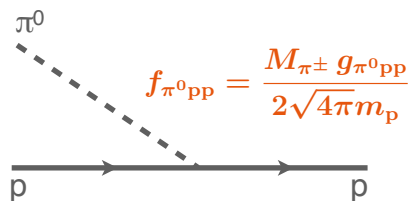
$$\begin{aligned} \sigma_{\text{tot}} &= 84.0_{[q^0]} - 10.2_{[q^2]} + 0.4_{[q^3]} - 0.4_{[q^4]} + 0.6_{[q^5]} - 0.0_{[q^6]} \\ &= 74.35(14)(17)(1) \text{ mb} \end{aligned}$$

truncation error (68% DoB) \longleftarrow \uparrow \longleftarrow uncertainty in the π N LECs
 statistical error (NN LECs) \longleftarrow \uparrow

5. Precision determination of pion-nucleon coupling constants

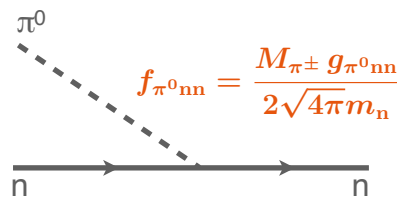
Patrick Reinert, Hermann Krebs, EE, Phys. Rev. Lett. 126 (2021) 9, 092501

- Fundamental observables that control the strength of the nuclear forces due to π -exchange
- Insights into isospin breaking at the hadronic/nuclear levels
- Gold-plated benchmarks for lattice-QCD + QED



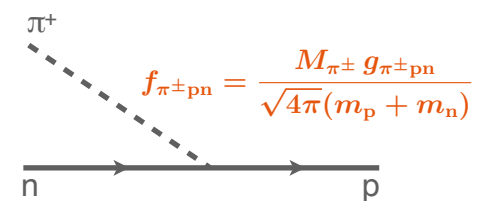
A Feynman diagram showing two protons (p) interacting via a neutral pion (π^0). A solid line with an arrow pointing right represents the incoming proton, and another solid line with an arrow pointing right represents the outgoing proton. A dashed line labeled π^0 connects the two vertices. The equation $f_{\pi^0 pp} = \frac{M_{\pi^\pm} g_{\pi^0 pp}}{2\sqrt{4\pi}m_p}$ is written above the diagram.

$$f_{\pi^0 pp} = \frac{M_{\pi^\pm} g_{\pi^0 pp}}{2\sqrt{4\pi}m_p}$$



A Feynman diagram showing two neutrons (n) interacting via a neutral pion (π^0). A solid line with an arrow pointing right represents the incoming neutron, and another solid line with an arrow pointing right represents the outgoing neutron. A dashed line labeled π^0 connects the two vertices. The equation $f_{\pi^0 nn} = \frac{M_{\pi^\pm} g_{\pi^0 nn}}{2\sqrt{4\pi}m_n}$ is written above the diagram.

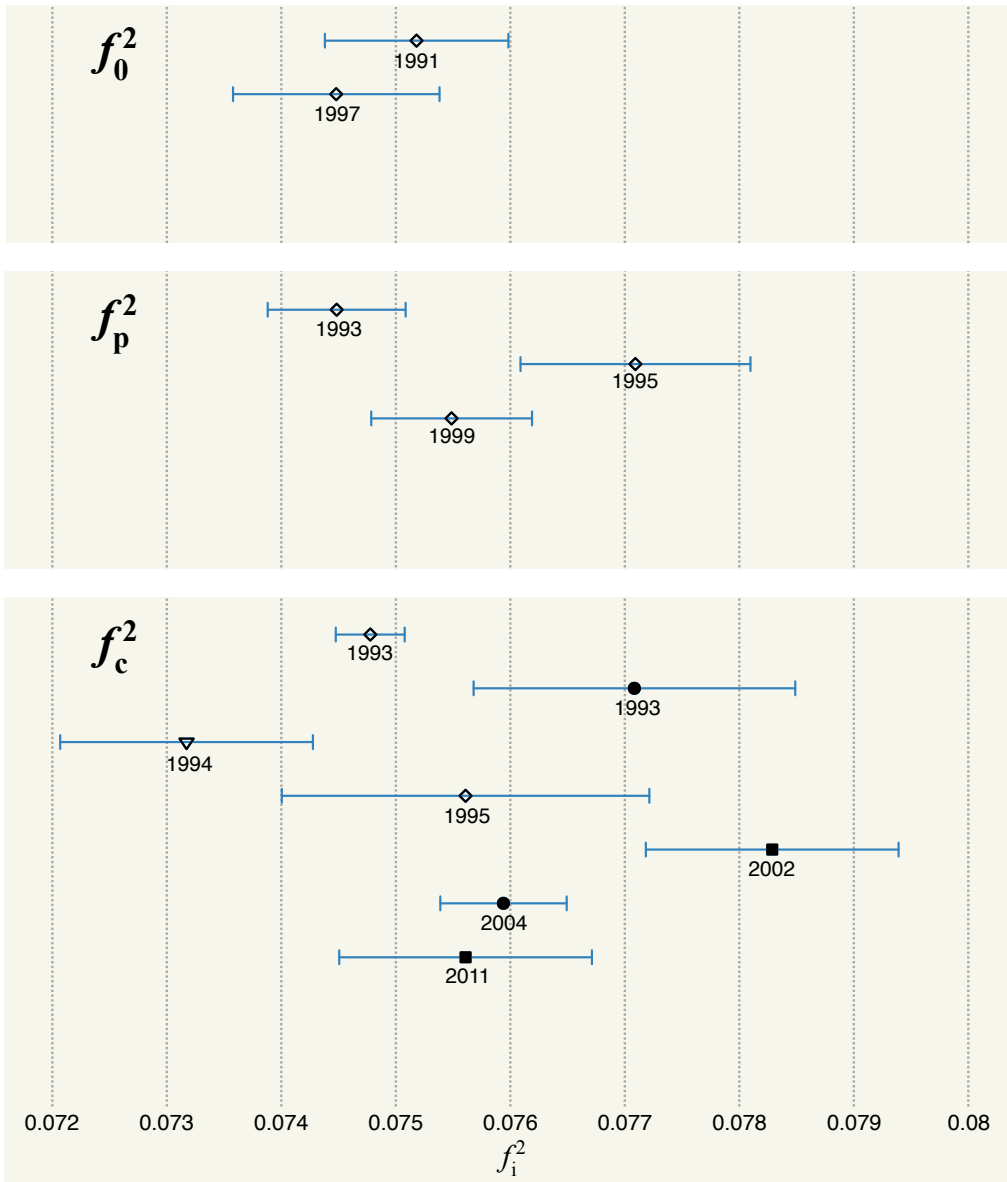
$$f_{\pi^0 nn} = \frac{M_{\pi^\pm} g_{\pi^0 nn}}{2\sqrt{4\pi}m_n}$$



A Feynman diagram showing a neutron (n) and a proton (p) interacting via a charged pion (π^+). A solid line with an arrow pointing right represents the incoming neutron, and another solid line with an arrow pointing right represents the outgoing proton. A dashed line labeled π^+ connects the two vertices. The equation $f_{\pi^\pm pn} = \frac{M_{\pi^\pm} g_{\pi^\pm pn}}{\sqrt{4\pi}(m_p + m_n)}$ is written above the diagram.

$$f_{\pi^\pm pn} = \frac{M_{\pi^\pm} g_{\pi^\pm pn}}{\sqrt{4\pi}(m_p + m_n)}$$

πN coupling constants: Some earlier determinations



Standard notation:

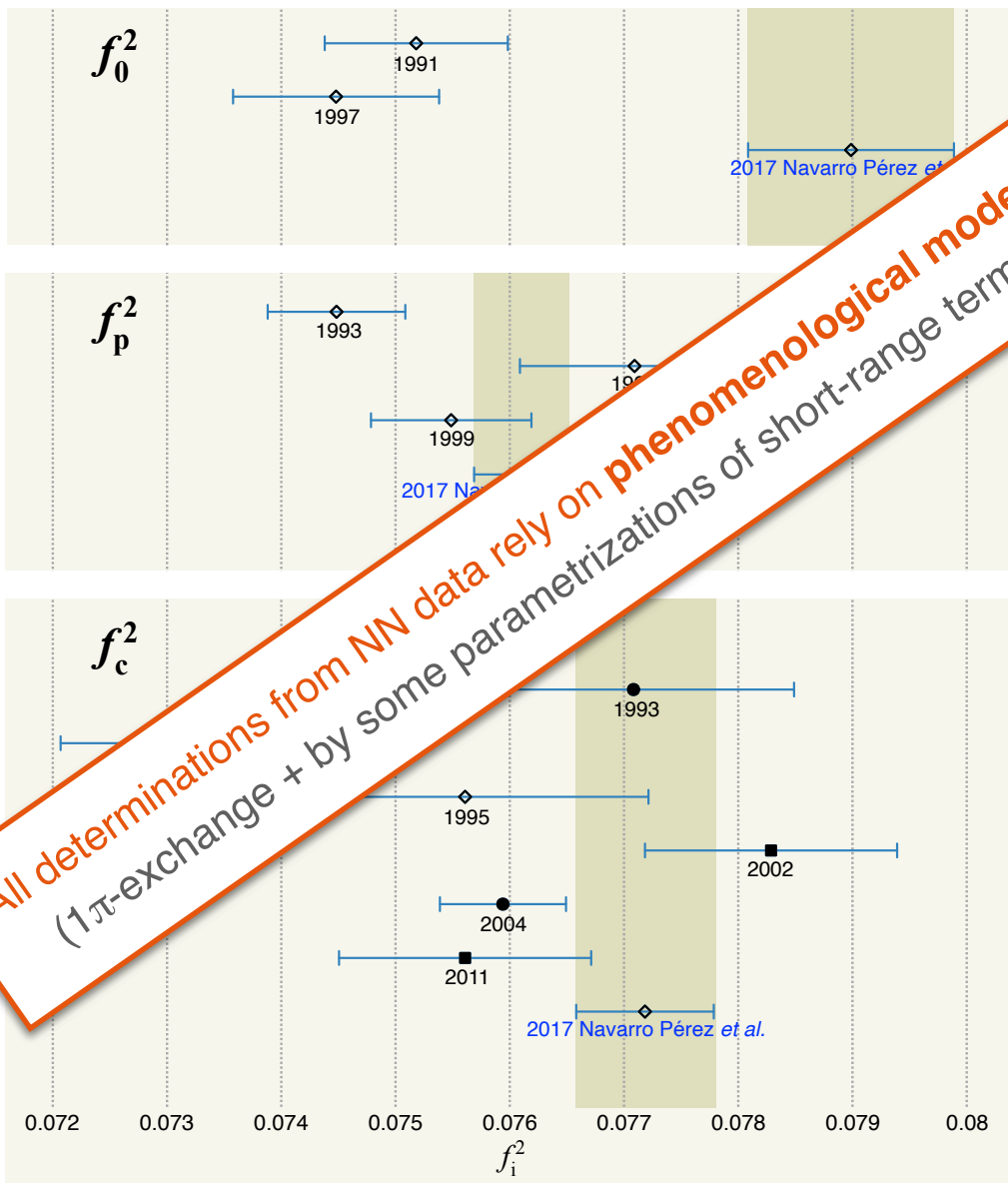
$$f_0^2 = -f_{\pi^0 nn} f_{\pi^0 pp}$$

$$f_p^2 = f_{\pi^0 pp} f_{\pi^0 pp}$$

$$2f_c^2 = f_{\pi^\pm pn} f_{\pi^\pm pn}$$

- — fixed-t dispersion relations of πN scattering
Markopoulou-Kalamara, Bugg '93; Arndt et al. '04
- — πN scattering lengths + Goldberger-Miyazawa-Oehme sum rule
Ericson et al. '02; Baru et al. '11
- ▼ — proton-antiproton PWA
Timmermans et al. '94
- ◇ — neutron-proton (+ proton-proton) PWA
Klomp et al. '91; Stoks et al. '93; Bugg et al. '95; de Swart et al. '97; Rentmeester et al. '99

πN coupling constants: Some earlier determinations



Standard notation:

$$f_0^2 = -f_{\pi^0 nn} f_{\pi^0 pp}$$

$$f_p^2 = f_{\pi^0 pp} f_{\pi^0 pp}$$

$$2f_c^2 = f_{\pi^\pm pn} f_{\pi^\pm pn}$$

- — fixed-t dispersion relations of πN scattering
Markopoulou-Kalamara, Bugg '93; Arndt et al. '04
- — πN scattering lengths + Goldberger-Miyazawa-Oehme sum rule
Ericson et al. '02; Baru et al. '11
- ▼ — proton-antiproton PWA
Timmermans et al. '94
- ◇ — neutron-proton (+ proton-proton) PWA
Klomp et al. '91; Stoks et al. '93; Bugg et al. '95; de Swart et al. '97; Rentmeester et al. '99

2017 Granada PWA: evidence for significant charge dependence of the coupling constants:

$$f_0^2 - f_p^2 = 0.0029(10)$$

Navarro Perez et al., PRC 95 (2017) 6, 064001

Anatomy of the calculation

The goal: *Bayesian* determination of f_c^2 , f_p^2 and f_0^2 by performing a full-fledged PWA of NN data up to pion-production threshold in the framework of chiral EFT

1. Experimental data:

- About 8000 published np and pp scattering data below $E_{\text{lab}} = 350$ MeV. Not all data are mutually compatible...
- Selections of mutually compatible data: Nijmegen 1993, Granada 2013, 2017
- **Performed own selection of compatible data** (found some differences to Granada...)

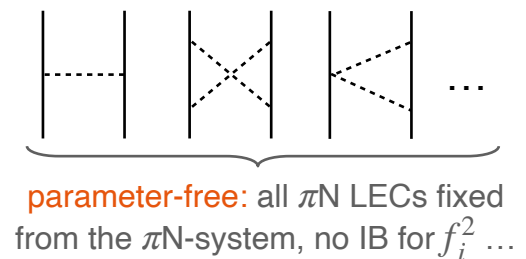
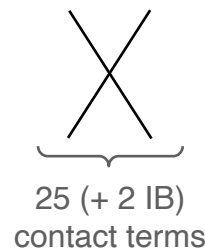
2. Interaction model:

- Long-range EM interactions (included in all PWA...)



- Semi-local chiral NN interaction at $N^4\text{LO}^+$ from P. Reinert, H. Krebs, EE, EPJA 54 (2018) 88

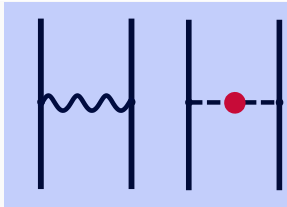
The treatment of isospin-breaking (IB) contributions was incomplete (limited to that of Nijmegen/Granada PWA)



We now include all charge-independence & charge-symmetry-breaking terms to $N^4\text{LO}$.

Isospin-breaking NN forces

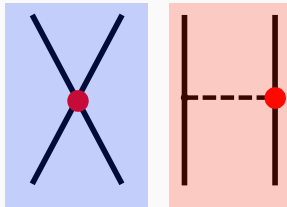
NLO



Have been employed in Reinert, Krebs, EE, EPJA 54 (2018) 88

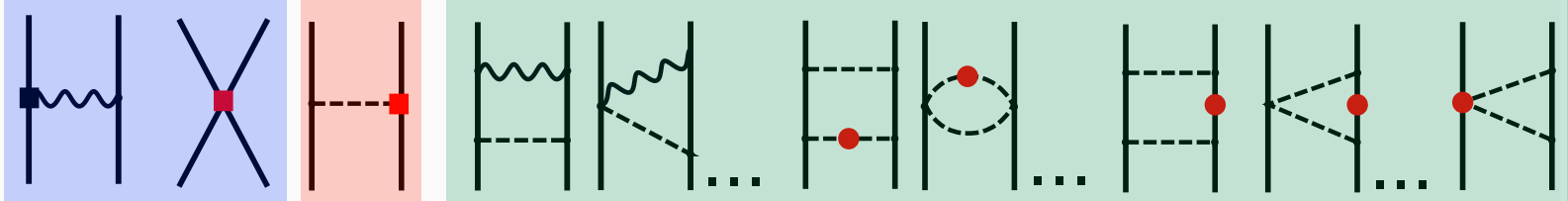
Parameter-free: depend on δM_π , $\delta m = 1.29$ MeV and $(\delta m)^{\text{QCD}} = 2.05(30)$ MeV [Gasser, Leutwyler '75]

N²LO

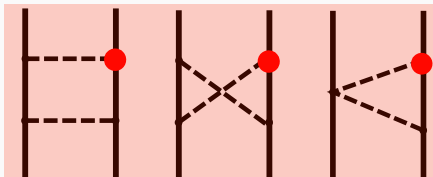
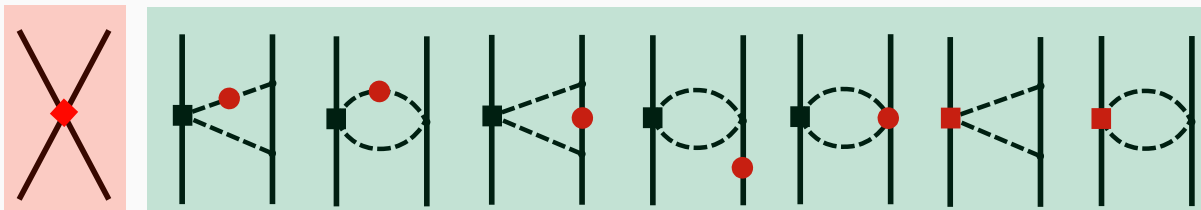


Depend on 3 πN coupling constants + 3 IB contact terms in p-waves

N³LO



N⁴LO



van Kolck et al. '98; Friar et al. '99, '03, '04; Niskanen '02; EE, Meißner '05

Determination of the πN constants

Free parameters: 3 πN LECs $f^2 \equiv \{f_c^2, f_p^2, f_0^2\}$, the 25 IC + 5 IB LECs C and the cutoff Λ .

$$p(f^2|D) = \int d\Lambda dC p(f^2 C \Lambda | D) = \int d\Lambda dC \frac{p(D|f^2 C \Lambda) p(f^2 C \Lambda)}{p(D)}$$

↑ NN data (to be specified later)
↑ use Bayes' theorem
↑ just a normalization constant

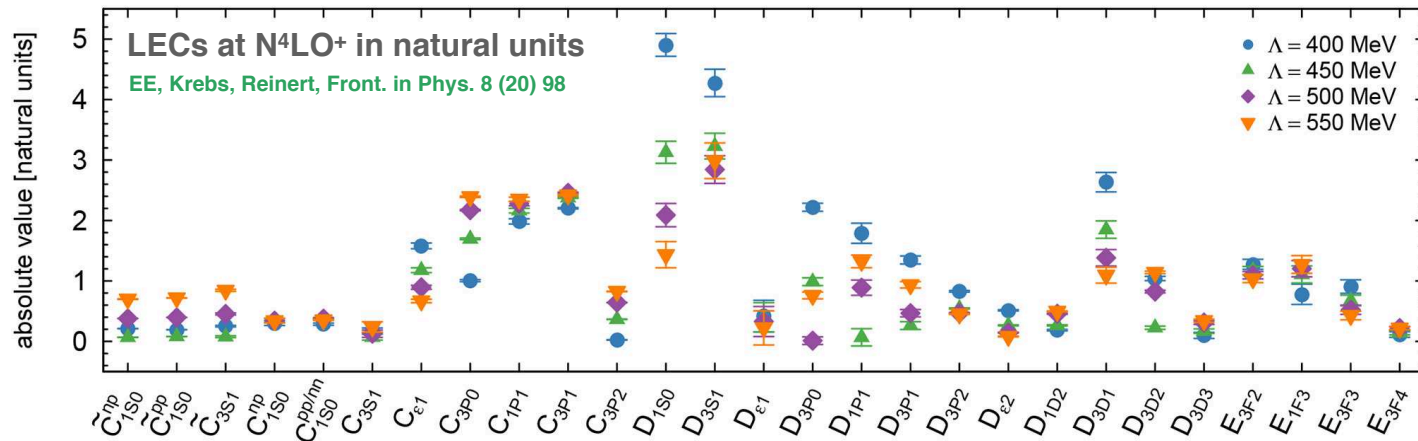
For normally distributed errors, the likelihood of data D is given by $p(D|f^2 C \Lambda) = \frac{1}{N} e^{-\frac{1}{2}\chi^2}$

Employ independent priors: $p(f^2 C \Lambda) = p(f^2) p(C) p(\Lambda)$

$p(f^2)$ — uniform prior (cuboid) to cover the range of possible values of f^2

$p(\Lambda)$ — uniform prior for $\Lambda \in [400 \text{ MeV}, 550 \text{ MeV}]$ (to be justified later)

$p(C)$ — multivariate Gaussian: $p(C) = (\sqrt{2\pi\bar{C}})^{-30} \exp(-\bar{C}^2/(2\bar{C}^2))$ with $\bar{C} = 5$



Determination of the πN constants

Free parameters: 3 πN LECs $f^2 \equiv \{f_c^2, f_p^2, f_0^2\}$, the 25 IC + 5 IB LECs C and the cutoff Λ .

$$p(f^2|D) = \int d\Lambda dC p(f^2 C \Lambda | D) = \int d\Lambda dC \frac{p(D|f^2 C \Lambda) p(f^2 C \Lambda)}{p(D)}$$

↑ NN data (to be specified later)
↑ use Bayes' theorem
↑ just a normalization constant

For normally distributed errors, the likelihood of data D is given by $p(D|f^2 C \Lambda) = \frac{1}{N} e^{-\frac{1}{2}\chi^2}$

Thus, need to evaluate a 30 (C) + 1 (Λ) dimensional integral at $\sim 10^3$ grid points for f^2 ... 🤔

Solution: Use the Laplace approximation by approximating the likelihood $p(D|f^2 C \Lambda)$ via :

$$p(D|f^2 C \Lambda) \approx \frac{1}{N} e^{-\frac{1}{2}[\chi_{\min}^2 + \frac{1}{2}(C - C_{\min})^T H (C - C_{\min})]}$$

where $\chi_{\min}^2 \equiv \chi_{\min}^2(f^2, \Lambda)$ at $C_{\min} \equiv C_{\min}(f^2, \Lambda)$ and $H_{ij}(f^2, \Lambda) = \left. \frac{\partial^2 \chi^2}{\partial C_i \partial C_j} \right|_{C=C_{\min}}$.

Then:

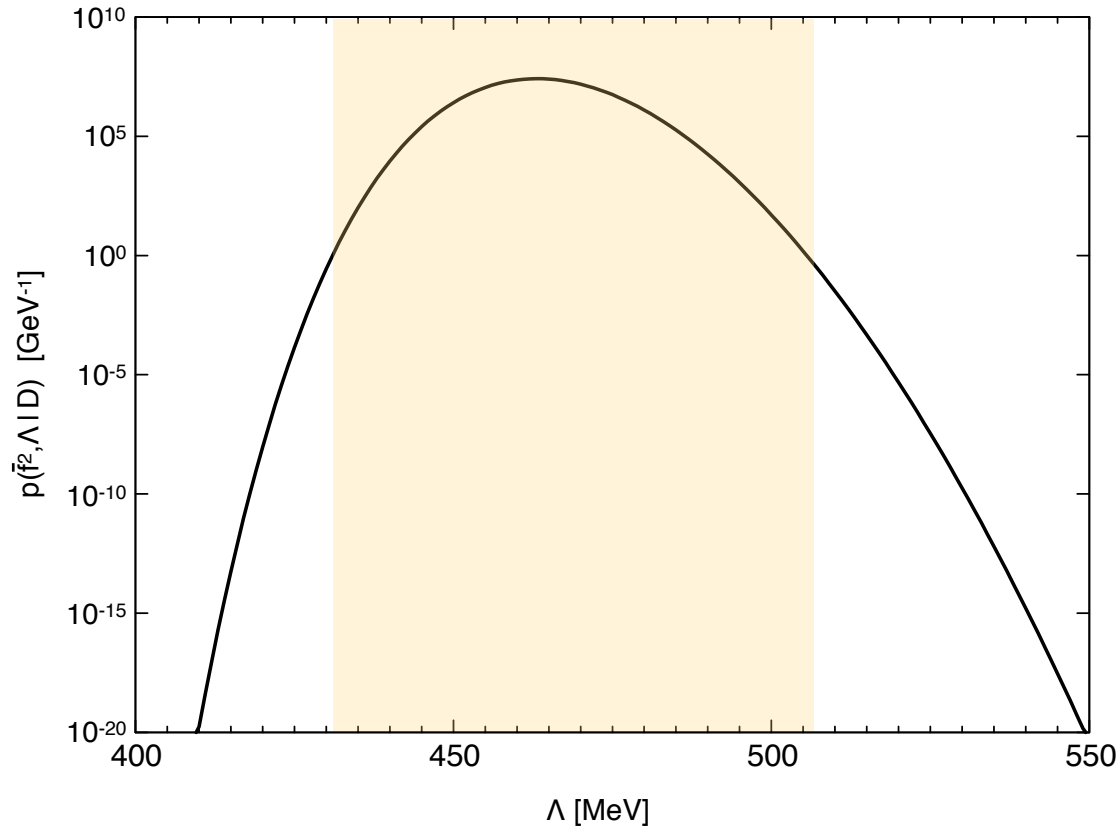
$$p(f^2|D) = \frac{1}{\tilde{N}} \int_{\Lambda_{\min}}^{\Lambda_{\max}} d\Lambda \frac{1}{\sqrt{\det A}} e^{-\frac{1}{2}(\chi_{\min}^2 + \frac{1}{\bar{C}^2} C_{\min}^T C_{\min} - \frac{1}{\bar{C}^4} C_{\min}^T A^{-1} C_{\min})} \underbrace{\mathbb{1}_B(f^2)}_{\text{the indicator function for } f^2}$$

$A = 1/2H + 1/\bar{C}^2 \mathbb{1}$

still requires $\sim 10^4$ determinations of 30 LECs C from NN data...

Determination of the πN constants

How does the integrand look like for some typical values f^2 ?



This shows that the employed prior $p(\Lambda)$ is indeed uninformative...

Then:

$$p(f^2 | D) = \frac{1}{\tilde{N}} \int_{\Lambda_{\min}}^{\Lambda_{\max}} d\Lambda \frac{1}{\sqrt{\det A}} e^{-\frac{1}{2}(\chi_{\min}^2 + \frac{1}{\bar{C}^2} C_{\min}^T C_{\min} - \frac{1}{\bar{C}^4} C_{\min}^T A^{-1} C_{\min})} \underbrace{\mathbb{1}_B(f^2)}_{\text{the indicator function for } f^2}$$

$A = 1/2H + 1/\bar{C}^2 \mathbb{1}$

still requires $\sim 10^4$ determinations of 30 LECs C from NN data...

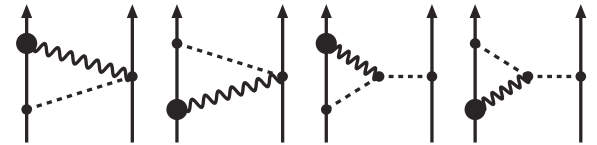
Error analysis

- Higher-order πN LECs c_i , d_i , e_i from the Roy-Steiner equation analysis: errors propagated using the covariance matrix provided in [Hoferichter et al., PRL 115 \(2015\) 192301](#).
- QCD contribution to $m_n - m_p$: used $(\delta m)^{\text{QCD}} = 2.05(30) \text{ MeV}$ [[Gasser, Leutwyler '75](#)] consistent with the lattice QCD+QED result $(\delta m)^{\text{QCD}} \sim 2.16 \text{ MeV}$ [[Borsanyi et al. '15](#)] and with the updated calc. $(\delta m)^{\text{QCD}} = 1.87(16) \text{ MeV}$ [[Gasser et al. '20](#)]. The resulting errors in f^2 are found to be negligible.
- Truncation of the chiral EFT expansion for IB interactions:

Model 1: IB terms up to N⁴LO

Model 2: same as model 1 + N⁵LO $\pi\gamma$ -exchange
(involve large isovector MM $\kappa_V = 4.7$)

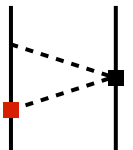
[Kaiser, PRC 73 \(2006\) 044001](#)



Model 3: same as model 1 + N⁵LO 2π -exchange proportional to $(f_i - f_j)c_k$

$$V^{(6)}(q) = -\frac{f_c(2f_c - f_p - f_n)c_4}{4F_\pi^2 M_{\pi^\pm}^2} \tau_1^3 \tau_2^3 (\vec{\sigma}_1 \cdot \vec{q} \vec{\sigma}_2 \cdot \vec{q} - q^2 \vec{\sigma}_1 \cdot \vec{\sigma}_2) (4M_\pi^2 + q^2) A(q)$$

$$- \frac{f_c(f_p - f_n)}{2F_\pi^2 M_{\pi^\pm}^2} (\tau_1^3 + \tau_2^3) (2M_\pi^2 + q^2) (4M_\pi^2 c_1 - c_3(2M_\pi^2 + q^2)) A(q)$$



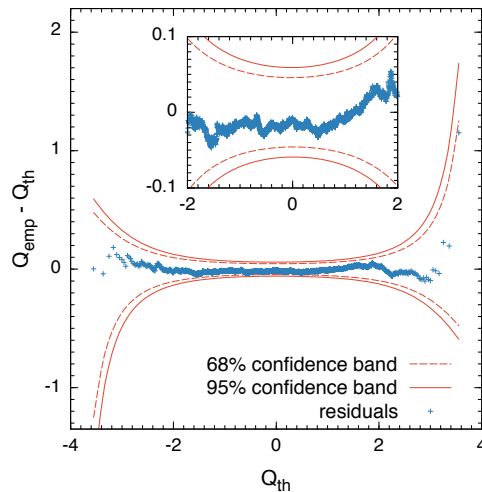
Calculate $p(f^2|D)$ using the Models 1-3 and perform (Bayesian) averaging at the end.

Error analysis

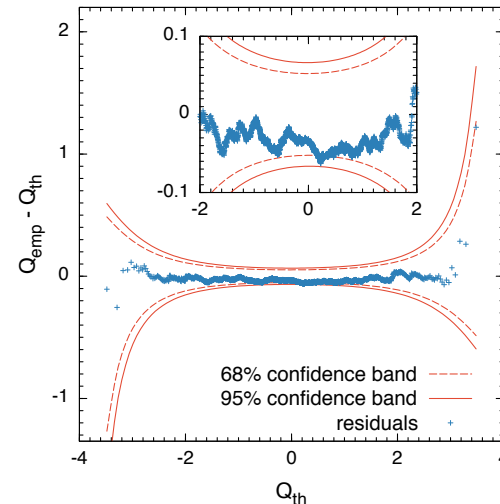
- **Experimental data:** performed own recursive selection of mutually compatible np, pp data using the standard 3σ -criterion (found some differences with the Granada 2013 database).
- Setting the energy range $[0, E_{\max}]$ for the included NN data:
 - higher E_{\max} : more data available 😊 but lower accuracy of the EFT... 😞
 - lower E_{\max} : high accuracy of the EFT 😊 but less data & possible overfitting... 😞

To avoid possible overfitting performed statistical consistency tests by verifying the normal distribution of residuals (tail sensitive test by Aldor-Noiman et al. *Am. Stat.* 67 (2013) 249)

Rotated quantile-quantile plot for $E_{\max} = 300$ MeV

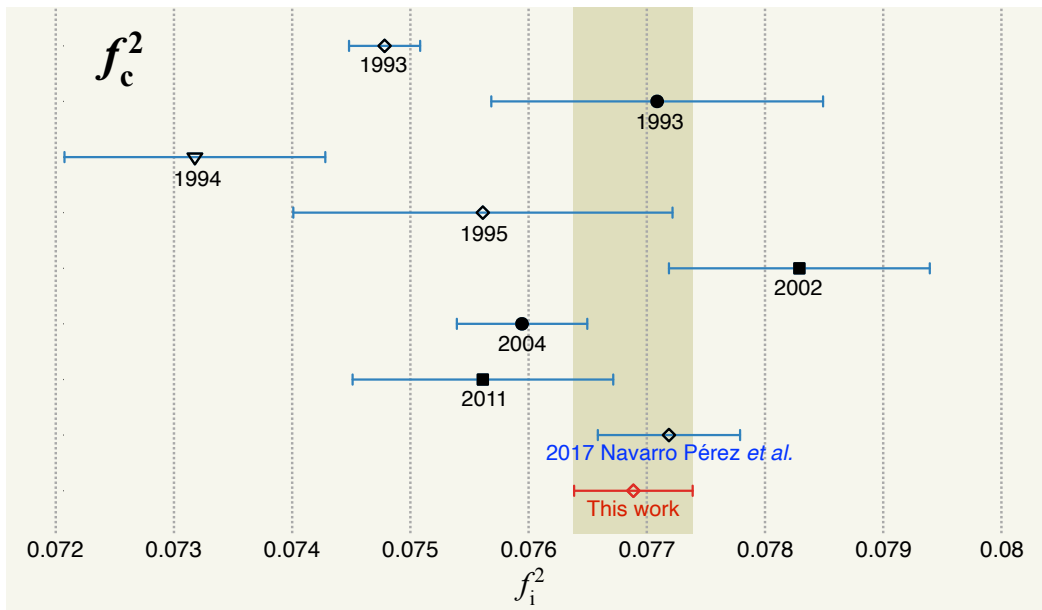
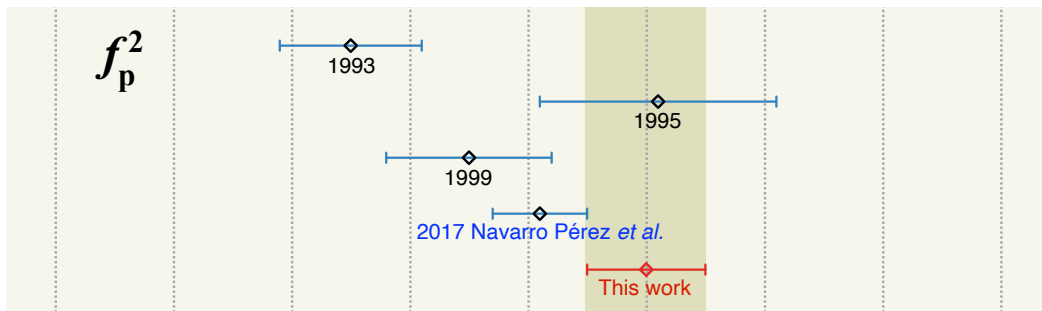
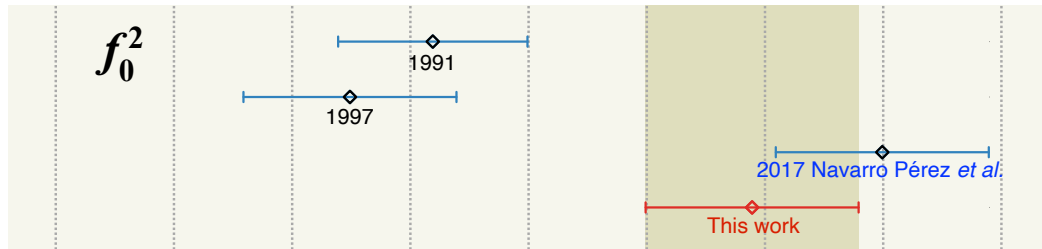


Rotated quantile-quantile plot for $E_{\max} = 220$ MeV



To stay unbiased, average over independent analyses for $E_{\max} = 300, 280, \dots, 220$ MeV

Determination of the πN constants



Our result:

$$f_0^2 = 0.0779(9)(1.3)$$

$$f_p^2 = 0.0770(5)(0.8)$$

$$f_c^2 = 0.0769(5)(0.9)$$

statistical and systematic errors due to the EFT truncation, choice of E_{\max} and data selection

uncertainty in the subleading πN LECs

Our f_c^2 value is consistent with the extractions from the πN system

Contrary to the Granada group, we see **no evidence for charge dependence** of the πN coupling constants

Using the PDG-2020 value for the axial charge $g_A = 1.2756(13)$, the GT discrepancy amounts to (f_c):

$$\Delta_{GT} \sim 1.7\%$$

Determination of the πN constants

Our $g_{\pi NN}$ value corresponding to f_c^2 reads:

$$g_{\pi NN} = 13.92 \pm 0.09$$

Pionic hydrogen exp. at PSI (GMO sum rule)

[Hirtl et al., Eur. Phys. J. A57 (2021) 2, 70]

$$\epsilon_{1s}^{\pi H} + \epsilon_{1s}^{\pi D} : g_{\pi NN} = 13.66 \pm 0.20$$

$$\Gamma_{1s}^{\pi H} : g_{\pi NN} = 13.96 \pm 0.22$$

Our result:

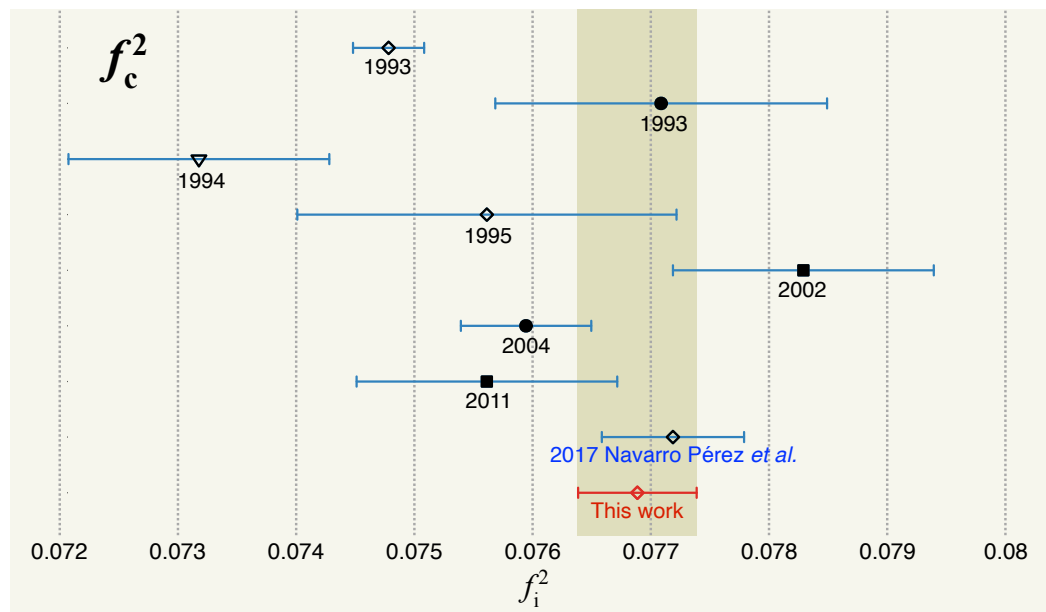
$$f_0^2 = 0.0779(9)(1.3)$$

$$f_p^2 = 0.0770(5)(0.8)$$

$$f_c^2 = 0.0769(5)(0.9)$$

statistical and systematic errors due to the EFT truncation, choice of E_{\max} and data selection

uncertainty in the subleading πN LECs



Our f_c^2 value is consistent with the extractions from the πN system

Contrary to the Granada group, we see **no evidence for charge dependence** of the πN coupling constants

Using the PDG-2020 value for the axial charge $g_A = 1.2756(13)$, the GT discrepancy amounts to (f_c):

$$\Delta_{GT} \sim 1.7\%$$

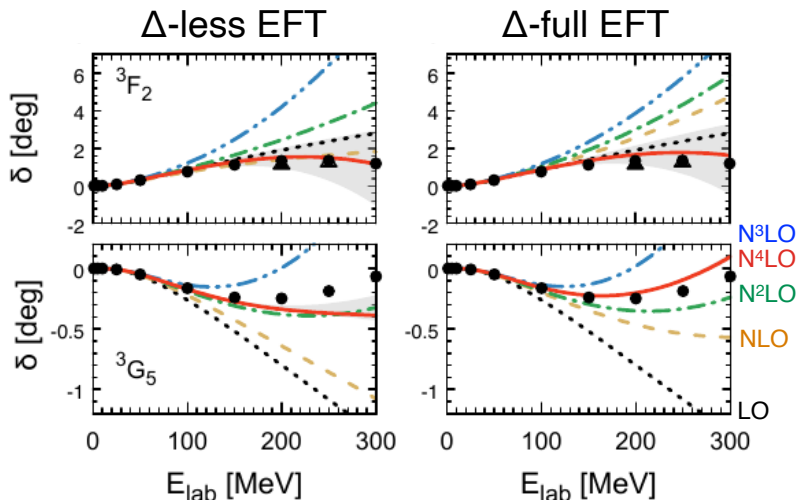
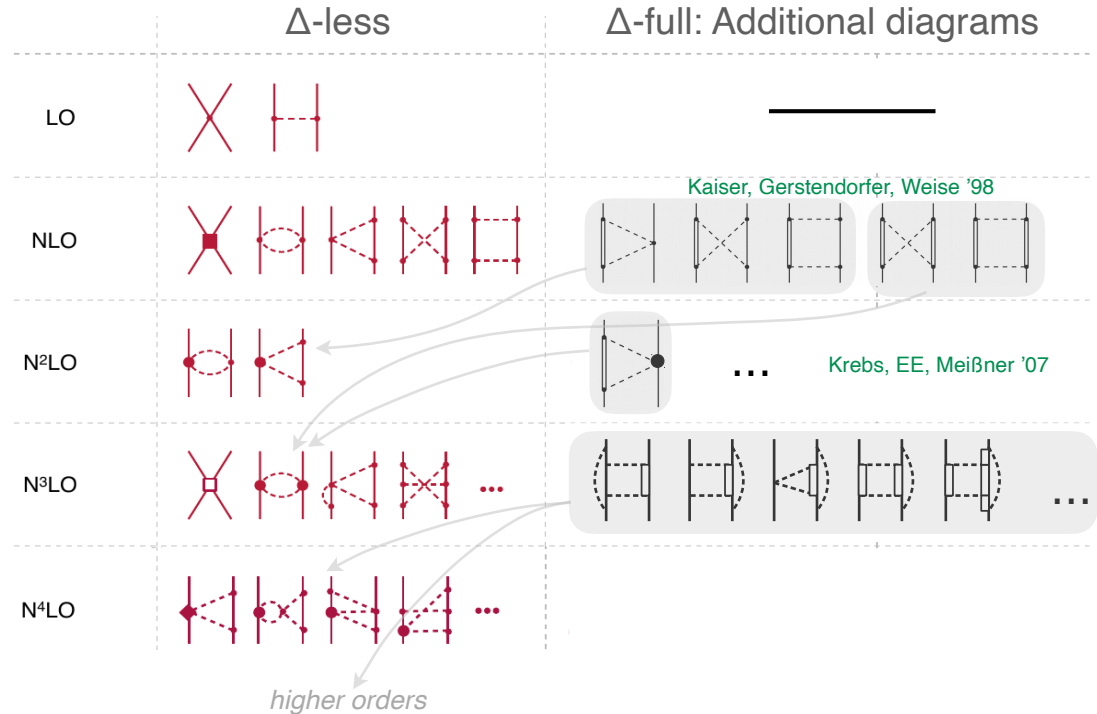
Chiral EFT with explicit $\Delta(1232)$

Motivation:

- treating Δ as an explicit DoF allows one to resum $(m_\Delta - m_N)^{-n}$ corrections
- superior performance of Δ -EFT@N²LO for heavy nuclei Ekström et al. '18

Results:

- Δ -contributions to the TPEP upto N²LO known: **improved convergence**
- peripheral NN scattering (Born approx.): hints of a slightly improved convergence but similar results at the highest order A. Gasparyan, H. Krebs, EE, in preparation



Next steps:

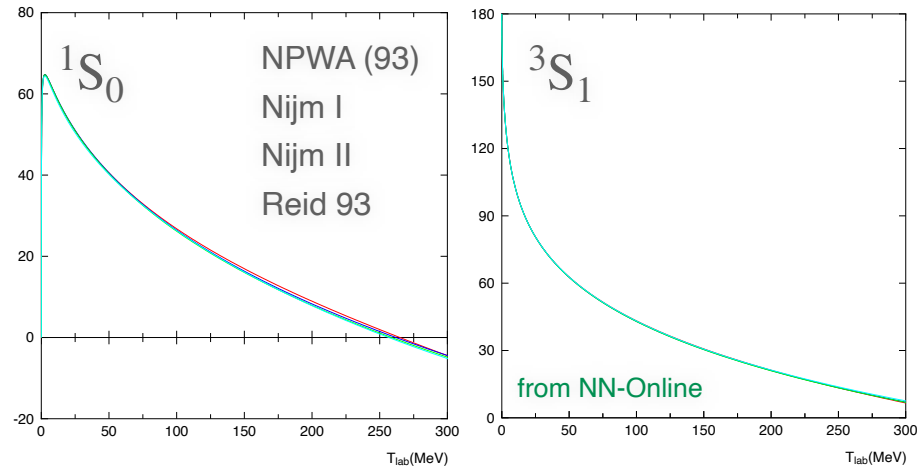
- three-pion exchange potential using the method of UT [work in progress by **Victor Springer**]
- fit the NN LECs to np + pp scattering data and test the resulting potentials in few-N systems

The 3NF challenge

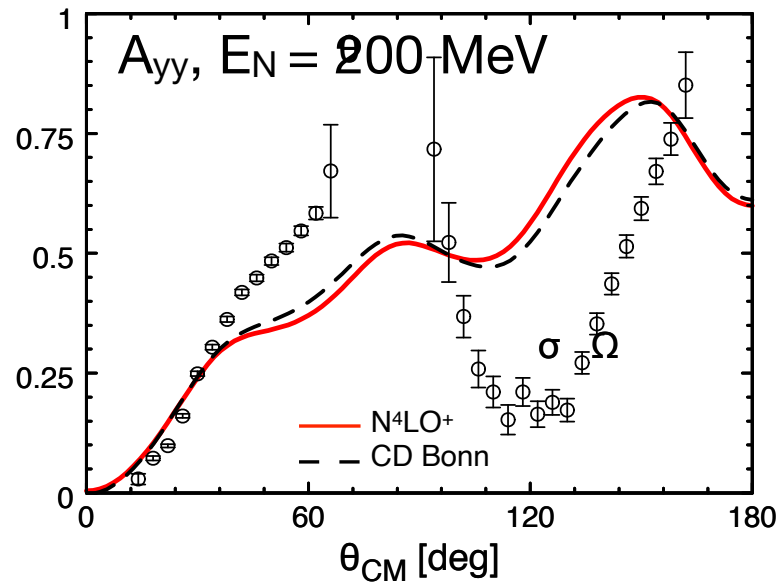
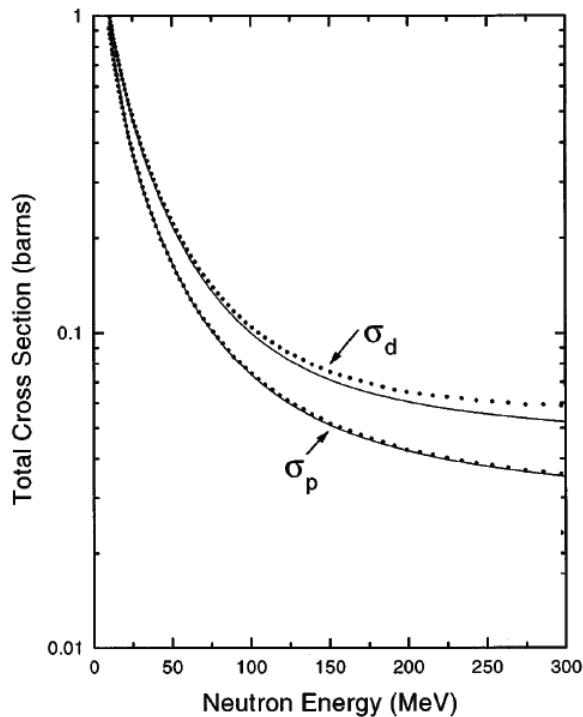
1. Introduction

Since the 90-es, we know that:

- 2N force is easy to parametrize:
2 (isospin) \times 6 spin-momentum operators
- after removing inconsistent data ($\sim 10\%$ pp and $\sim 30\%$ np...), the rest of the data base can be described with $\chi^2/\text{datum} \sim 1$.



While the NN forces seem under control, large deviations show up for Nd scattering signaling the missing 3N forces

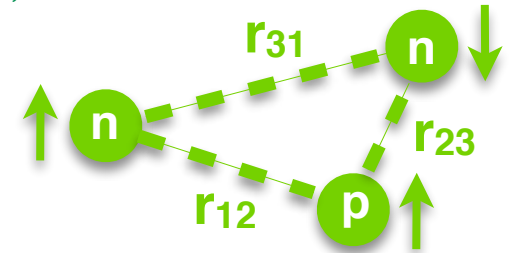


1. Introduction

The most general structure of a local, isospin-symmetric 3NF

Krebs, Gasparyan, EE '13; Phillips, Schat '13; EE, Gasparyan, Krebs, Schat '15

Generators \mathcal{G} in momentum space	Generators $\tilde{\mathcal{G}}$ in coordinate space
$\mathcal{G}_1 = 1$	$\tilde{\mathcal{G}}_1 = 1$
$\mathcal{G}_2 = \boldsymbol{\tau}_1 \cdot \boldsymbol{\tau}_3$	$\tilde{\mathcal{G}}_2 = \boldsymbol{\tau}_1 \cdot \boldsymbol{\tau}_3$
$\mathcal{G}_3 = \vec{\sigma}_1 \cdot \vec{\sigma}_3$	$\tilde{\mathcal{G}}_3 = \vec{\sigma}_1 \cdot \vec{\sigma}_3$
$\mathcal{G}_4 = \boldsymbol{\tau}_1 \cdot \boldsymbol{\tau}_3 \vec{\sigma}_1 \cdot \vec{\sigma}_3$	$\tilde{\mathcal{G}}_4 = \boldsymbol{\tau}_1 \cdot \boldsymbol{\tau}_3 \vec{\sigma}_1 \cdot \vec{\sigma}_3$
$\mathcal{G}_5 = \boldsymbol{\tau}_2 \cdot \boldsymbol{\tau}_3 \vec{\sigma}_1 \cdot \vec{\sigma}_2$	$\tilde{\mathcal{G}}_5 = \boldsymbol{\tau}_2 \cdot \boldsymbol{\tau}_3 \vec{\sigma}_1 \cdot \vec{\sigma}_2$
$\mathcal{G}_6 = \boldsymbol{\tau}_1 \cdot (\boldsymbol{\tau}_2 \times \boldsymbol{\tau}_3) \vec{\sigma}_1 \cdot (\vec{\sigma}_2 \times \vec{\sigma}_3)$	$\tilde{\mathcal{G}}_6 = \boldsymbol{\tau}_1 \cdot (\boldsymbol{\tau}_2 \times \boldsymbol{\tau}_3) \vec{\sigma}_1 \cdot (\vec{\sigma}_2 \times \vec{\sigma}_3)$
$\mathcal{G}_7 = \boldsymbol{\tau}_1 \cdot (\boldsymbol{\tau}_2 \times \boldsymbol{\tau}_3) \vec{\sigma}_2 \cdot (\vec{q}_1 \times \vec{q}_3)$	$\tilde{\mathcal{G}}_7 = \boldsymbol{\tau}_1 \cdot (\boldsymbol{\tau}_2 \times \boldsymbol{\tau}_3) \vec{\sigma}_2 \cdot (\hat{r}_{12} \times \hat{r}_{23})$
$\mathcal{G}_8 = \vec{q}_1 \cdot \vec{\sigma}_1 \vec{q}_1 \cdot \vec{\sigma}_3$	$\tilde{\mathcal{G}}_8 = \hat{r}_{23} \cdot \vec{\sigma}_1 \hat{r}_{23} \cdot \vec{\sigma}_3$
$\mathcal{G}_9 = \vec{q}_1 \cdot \vec{\sigma}_3 \vec{q}_3 \cdot \vec{\sigma}_1$	$\tilde{\mathcal{G}}_9 = \hat{r}_{23} \cdot \vec{\sigma}_3 \hat{r}_{12} \cdot \vec{\sigma}_1$
$\mathcal{G}_{10} = \vec{q}_1 \cdot \vec{\sigma}_1 \vec{q}_3 \cdot \vec{\sigma}_3$	$\tilde{\mathcal{G}}_{10} = \hat{r}_{23} \cdot \vec{\sigma}_1 \hat{r}_{12} \cdot \vec{\sigma}_3$
$\mathcal{G}_{11} = \boldsymbol{\tau}_2 \cdot \boldsymbol{\tau}_3 \vec{q}_1 \cdot \vec{\sigma}_1 \vec{q}_1 \cdot \vec{\sigma}_2$	$\tilde{\mathcal{G}}_{11} = \boldsymbol{\tau}_2 \cdot \boldsymbol{\tau}_3 \hat{r}_{23} \cdot \vec{\sigma}_1 \hat{r}_{23} \cdot \vec{\sigma}_2$
$\mathcal{G}_{12} = \boldsymbol{\tau}_2 \cdot \boldsymbol{\tau}_3 \vec{q}_1 \cdot \vec{\sigma}_1 \vec{q}_3 \cdot \vec{\sigma}_2$	$\tilde{\mathcal{G}}_{12} = \boldsymbol{\tau}_2 \cdot \boldsymbol{\tau}_3 \hat{r}_{23} \cdot \vec{\sigma}_1 \hat{r}_{12} \cdot \vec{\sigma}_2$
$\mathcal{G}_{13} = \boldsymbol{\tau}_2 \cdot \boldsymbol{\tau}_3 \vec{q}_3 \cdot \vec{\sigma}_1 \vec{q}_1 \cdot \vec{\sigma}_2$	$\tilde{\mathcal{G}}_{13} = \boldsymbol{\tau}_2 \cdot \boldsymbol{\tau}_3 \hat{r}_{12} \cdot \vec{\sigma}_1 \hat{r}_{23} \cdot \vec{\sigma}_2$
$\mathcal{G}_{14} = \boldsymbol{\tau}_2 \cdot \boldsymbol{\tau}_3 \vec{q}_3 \cdot \vec{\sigma}_1 \vec{q}_3 \cdot \vec{\sigma}_2$	$\tilde{\mathcal{G}}_{14} = \boldsymbol{\tau}_2 \cdot \boldsymbol{\tau}_3 \hat{r}_{12} \cdot \vec{\sigma}_1 \hat{r}_{12} \cdot \vec{\sigma}_2$
$\mathcal{G}_{15} = \boldsymbol{\tau}_1 \cdot \boldsymbol{\tau}_3 \vec{q}_2 \cdot \vec{\sigma}_1 \vec{q}_2 \cdot \vec{\sigma}_3$	$\tilde{\mathcal{G}}_{15} = \boldsymbol{\tau}_1 \cdot \boldsymbol{\tau}_3 \hat{r}_{13} \cdot \vec{\sigma}_1 \hat{r}_{13} \cdot \vec{\sigma}_3$
$\mathcal{G}_{16} = \boldsymbol{\tau}_2 \cdot \boldsymbol{\tau}_3 \vec{q}_3 \cdot \vec{\sigma}_2 \vec{q}_3 \cdot \vec{\sigma}_3$	$\tilde{\mathcal{G}}_{16} = \boldsymbol{\tau}_2 \cdot \boldsymbol{\tau}_3 \hat{r}_{12} \cdot \vec{\sigma}_2 \hat{r}_{12} \cdot \vec{\sigma}_3$
$\mathcal{G}_{17} = \boldsymbol{\tau}_1 \cdot \boldsymbol{\tau}_3 \vec{q}_1 \cdot \vec{\sigma}_1 \vec{q}_3 \cdot \vec{\sigma}_3$	$\tilde{\mathcal{G}}_{17} = \boldsymbol{\tau}_1 \cdot \boldsymbol{\tau}_3 \hat{r}_{23} \cdot \vec{\sigma}_1 \hat{r}_{12} \cdot \vec{\sigma}_3$
$\mathcal{G}_{18} = \boldsymbol{\tau}_1 \cdot (\boldsymbol{\tau}_2 \times \boldsymbol{\tau}_3) \vec{\sigma}_1 \cdot \vec{\sigma}_3 \vec{\sigma}_2 \cdot (\vec{q}_1 \times \vec{q}_3)$	$\tilde{\mathcal{G}}_{18} = \boldsymbol{\tau}_1 \cdot (\boldsymbol{\tau}_2 \times \boldsymbol{\tau}_3) \vec{\sigma}_1 \cdot \vec{\sigma}_3 \vec{\sigma}_2 \cdot (\hat{r}_{12} \times \hat{r}_{23})$
$\mathcal{G}_{19} = \boldsymbol{\tau}_1 \cdot (\boldsymbol{\tau}_2 \times \boldsymbol{\tau}_3) \vec{\sigma}_3 \cdot \vec{q}_1 \vec{q}_1 \cdot (\vec{\sigma}_1 \times \vec{\sigma}_2)$	$\tilde{\mathcal{G}}_{19} = \boldsymbol{\tau}_1 \cdot (\boldsymbol{\tau}_2 \times \boldsymbol{\tau}_3) \vec{\sigma}_3 \cdot \hat{r}_{23} \hat{r}_{23} \cdot (\vec{\sigma}_1 \times \vec{\sigma}_2)$
$\mathcal{G}_{20} = \boldsymbol{\tau}_1 \cdot (\boldsymbol{\tau}_2 \times \boldsymbol{\tau}_3) \vec{\sigma}_1 \cdot \vec{q}_1 \vec{\sigma}_3 \cdot \vec{q}_3 \vec{\sigma}_2 \cdot (\vec{q}_1 \times \vec{q}_3)$	$\tilde{\mathcal{G}}_{20} = \boldsymbol{\tau}_1 \cdot (\boldsymbol{\tau}_2 \times \boldsymbol{\tau}_3) \vec{\sigma}_1 \cdot \hat{r}_{23} \vec{\sigma}_3 \cdot \hat{r}_{12} \vec{\sigma}_2 \cdot (\hat{r}_{12} \times \hat{r}_{23})$



80 operators generated by all possible permutations of **20 structures**:

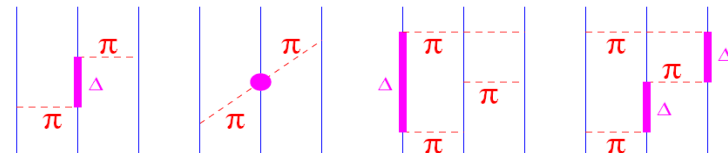
$$V(r_{12}, r_{23}, r_{31}) = \sum_{i=1}^{20} \tilde{\mathcal{G}}_i F_i(r_{12}, r_{23}, r_{31}) + \text{permutations}$$

$$V(q_1, q_2, q_3) = \sum_{i=1}^{20} \mathcal{G}_i F_i(q_1, q_2, q_3) + \text{permutations}$$

Nonlocal: 320 (!) operators
Topolnicki '17

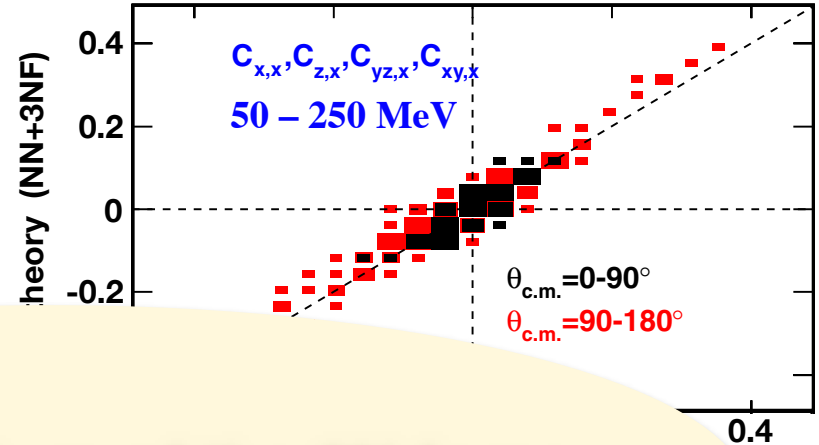
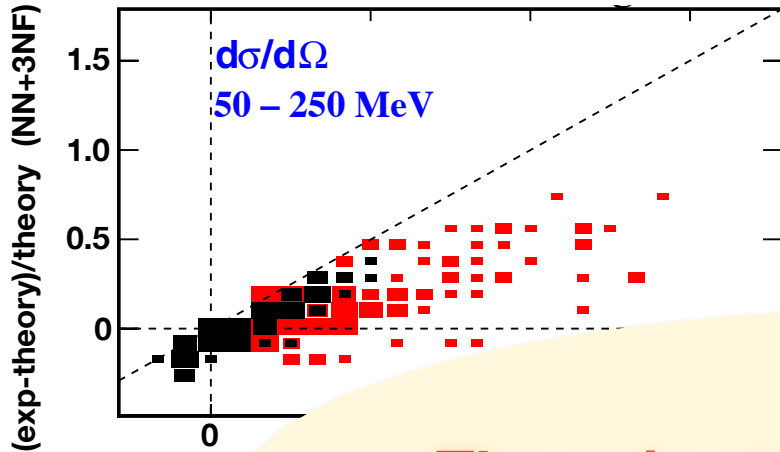
Phenomenological models:

Fujita-Miyazawa, Tucson-Melbourne,
Brasil, Urbana IX, Illinois, ...

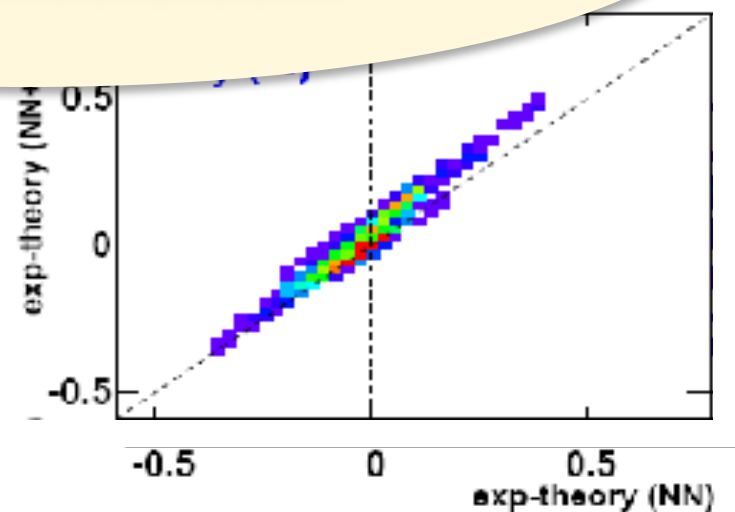
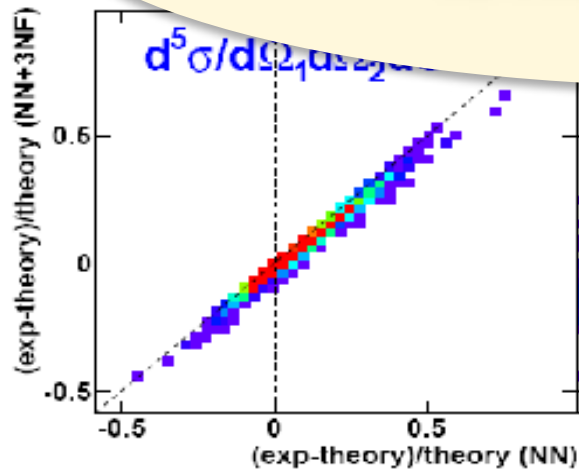


1. Introduction

Elastic nucleon-deuteron scattering



The spin structure of the 3N force
is NOT understood!

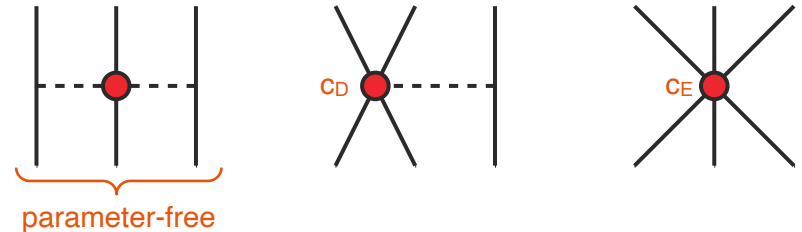


2. Inclusion of the 3NF at N²LO

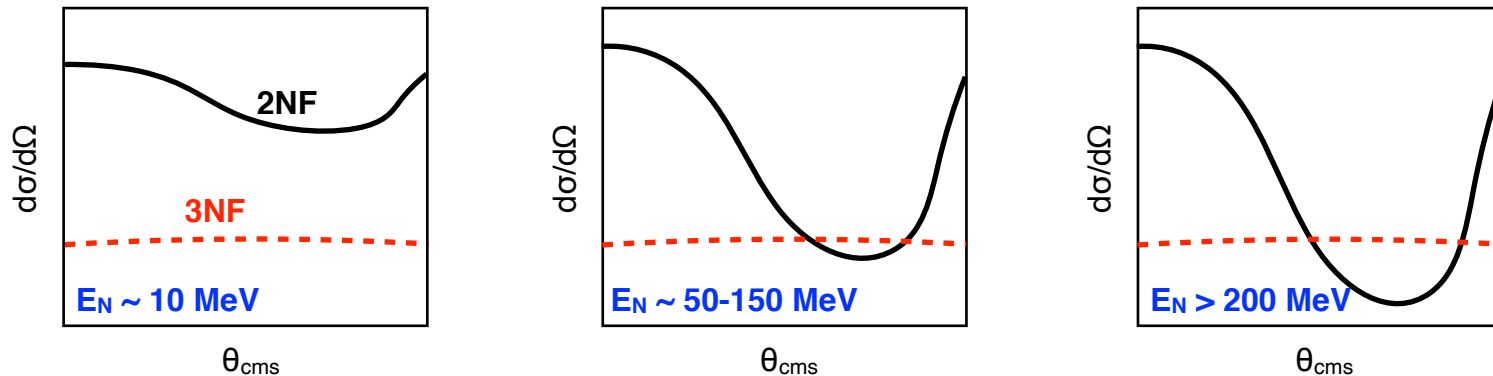
EE et al. [LENPIC], PRC99 (2019); Maris et al. [LENPIC], PRC103 (2021); e-Print: 2206.13303

The leading 3NF depends on 2 LECs that need to be determined from few-N data:

- ³H binding energy yields $c_E = f(c_D)$
- c_D is determined from Nd scattering



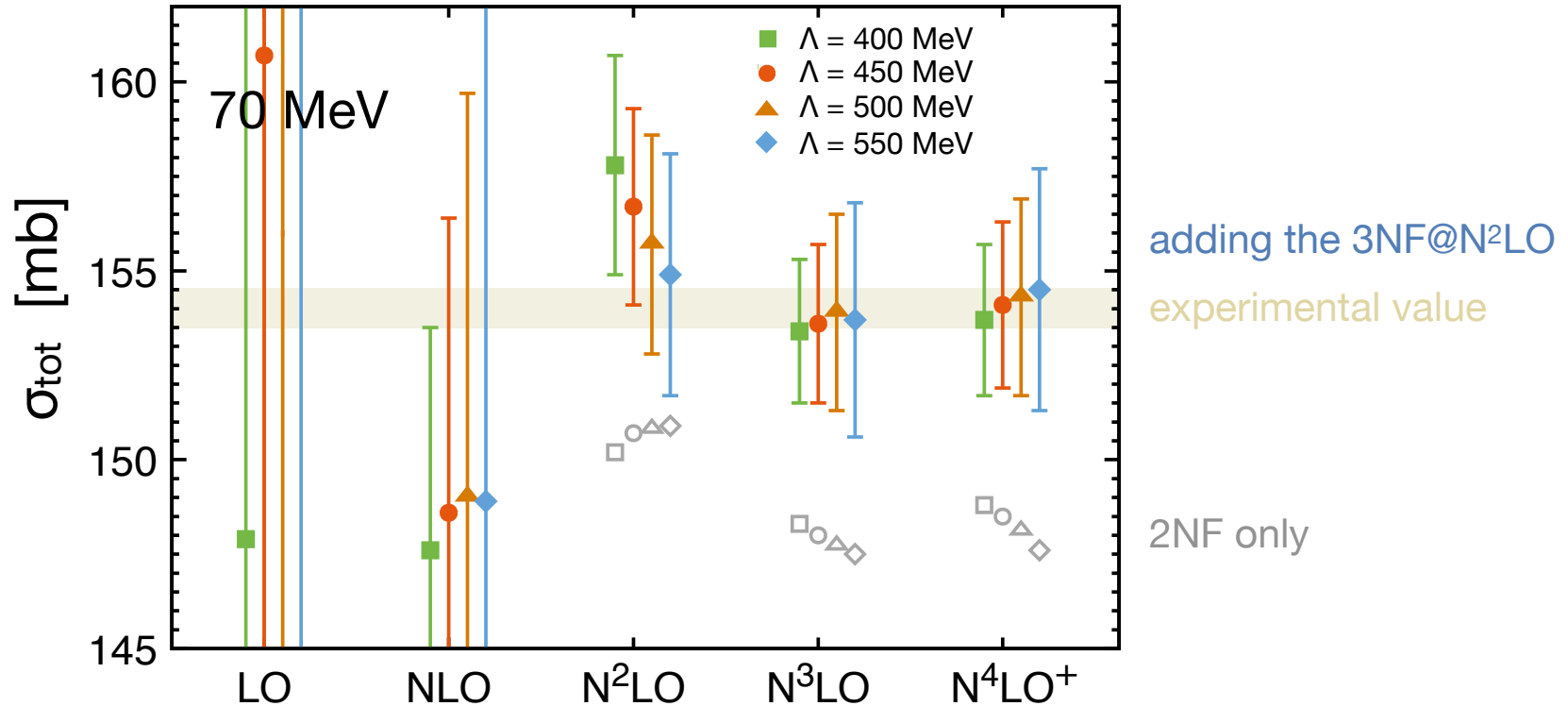
Differential cross section of Nd elastic scattering at intermediate and higher energies is known to be sensitive to the 3NF:



⇒ use precise Nd cross section data at 70 MeV from RIKEN [Kimiko Sekiguchi et al. '02] to fix c_D

2. Inclusion of the 3NF at N²LO

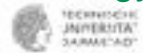
Maris et al. [LENPIC], e-Print: 2206.13303



- 2NF only underestimates the data; adding the 3NF improves the agreement with exp.
- 3NF contributions of natural size (W. counting)
- small residual cutoff dependence

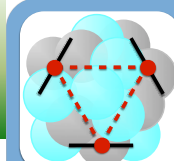


LENPIC: Low Energy Nuclear Physics International Collaboration

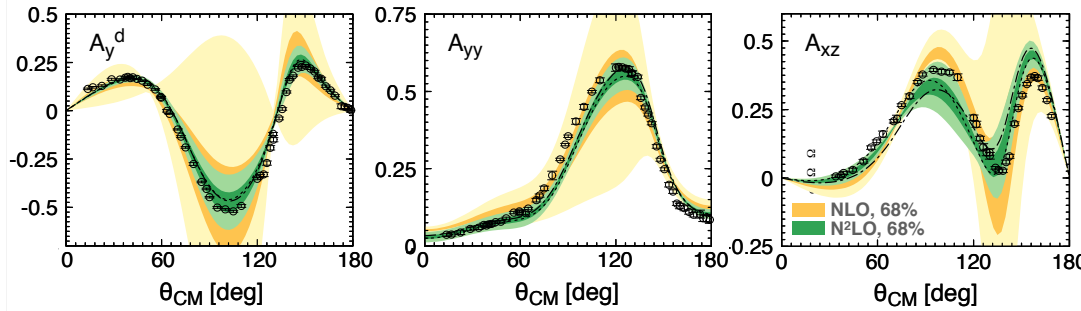


Few-N systems and light nuclei to N²LO

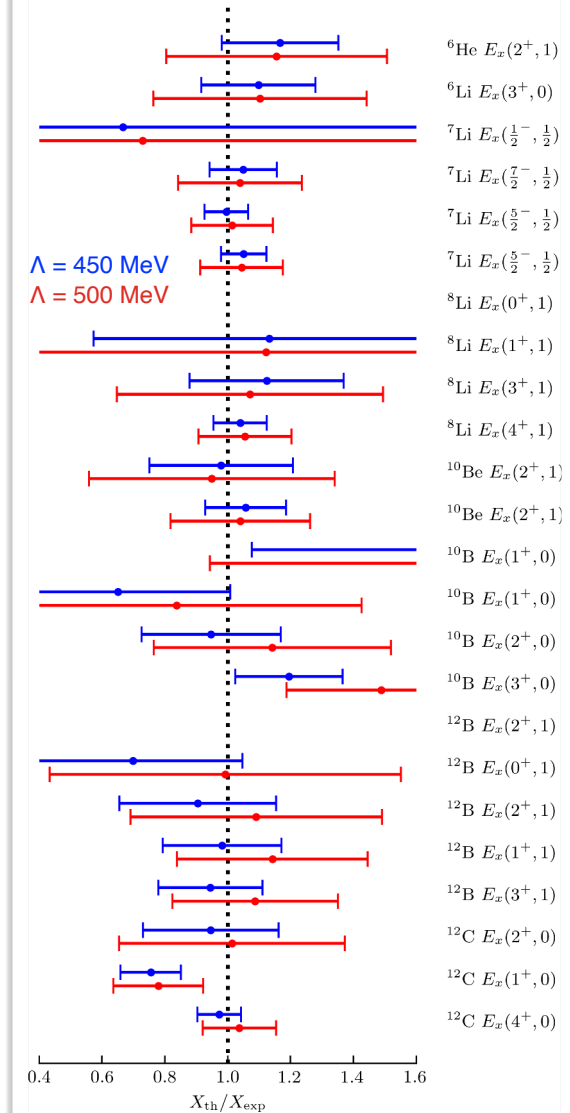
P. Maris et al. (LENPIC), Phys. Rev. C 103 (2021) 5, 054001



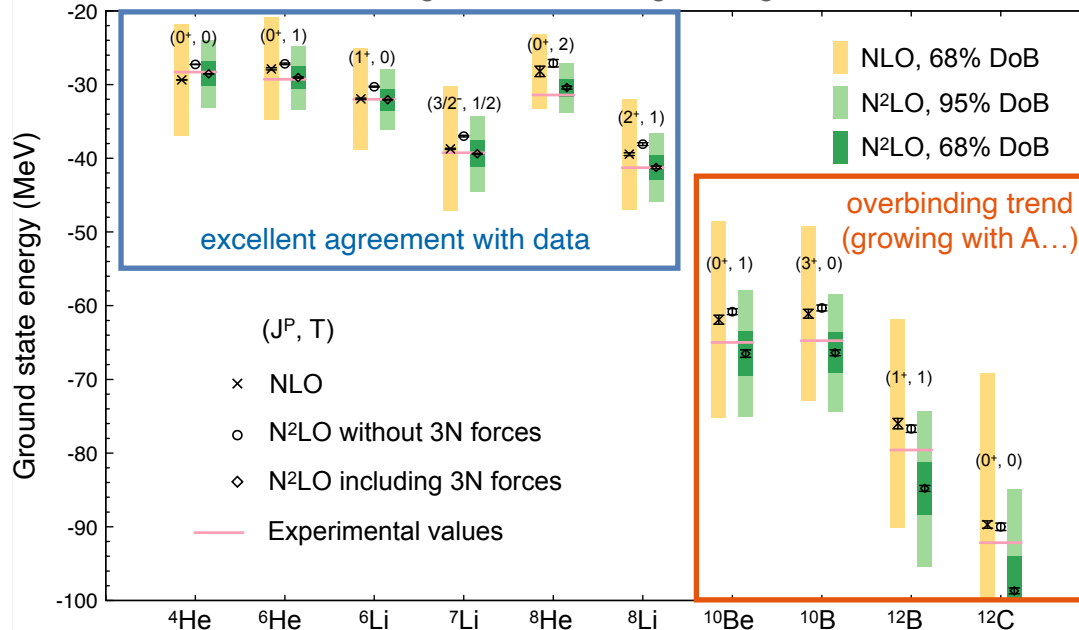
Tensor analyzing powers in Nd elastic scattering at 70 MeV



Excitation energies

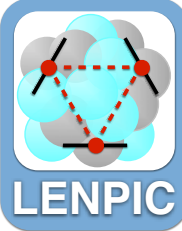


Predictions for ground-state energies of light nuclei

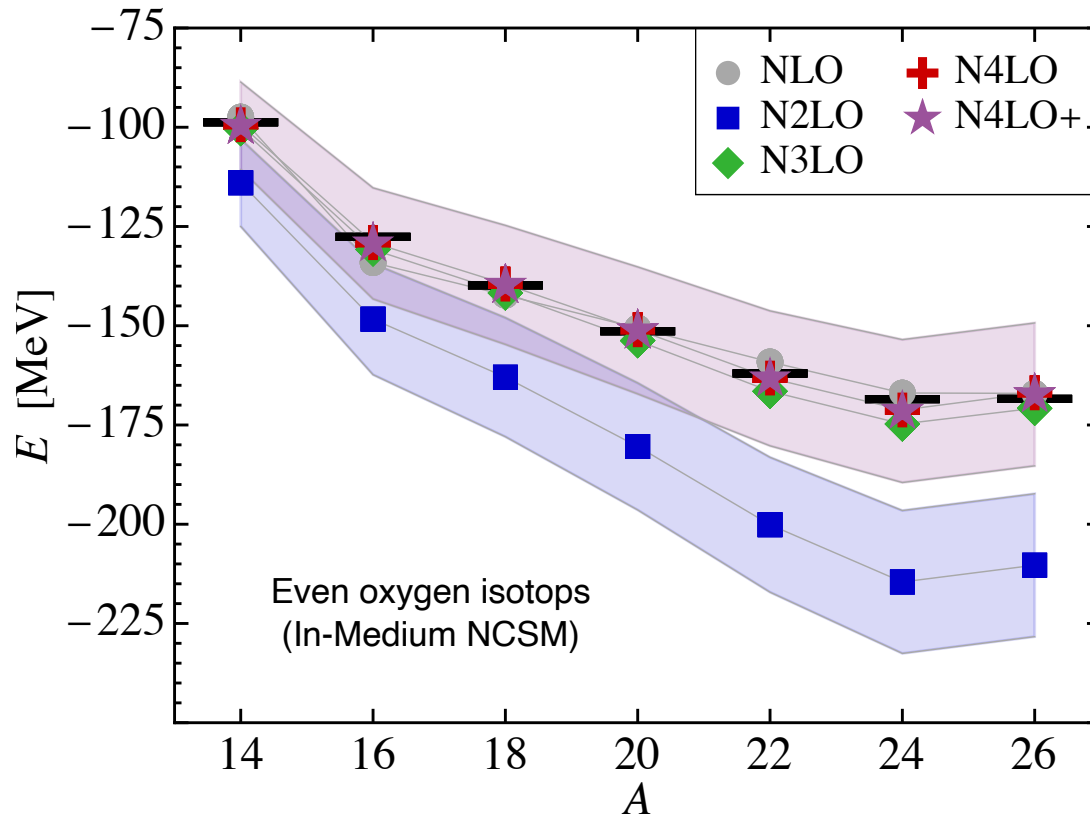


Few-N systems and light nuclei to N²LO

P. Maris et al. (LENPIC), e-Print: 2206.13303 [nucl-th]



A remarkable predictive power!

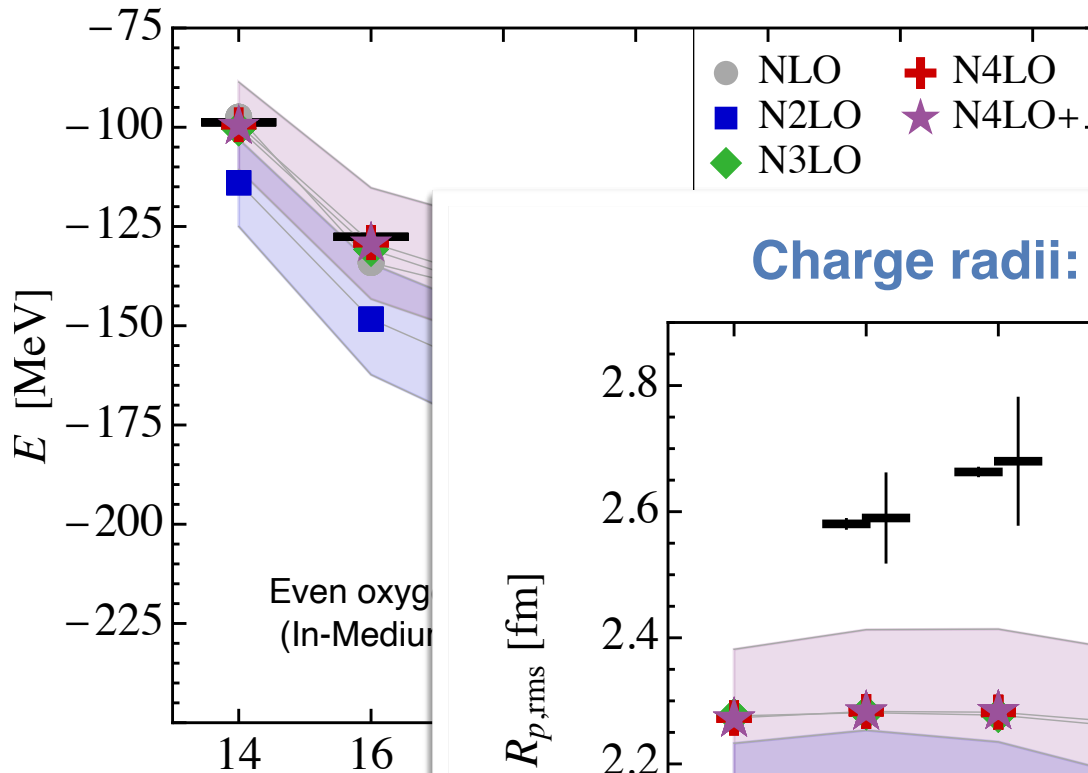


Few-N systems and light nuclei to N²LO

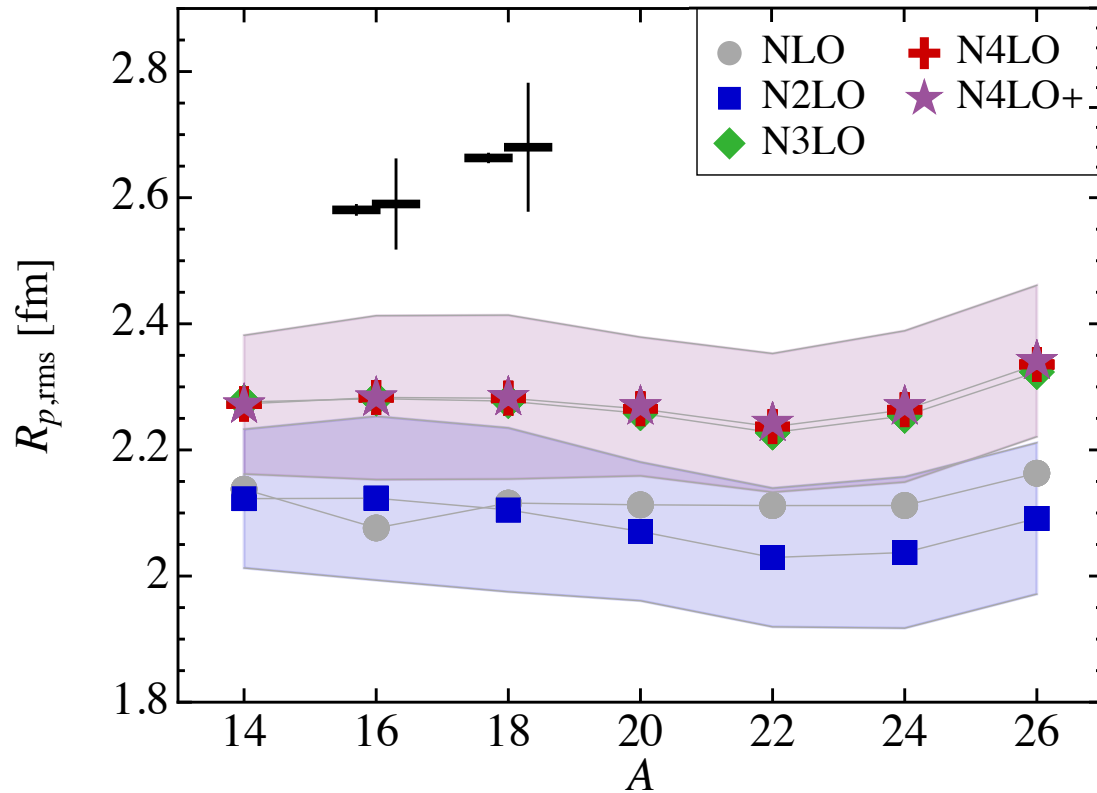
P. Maris et al. (LENPIC), e-Print: 2206.13303 [nucl-th]



A remarkable predictive power!



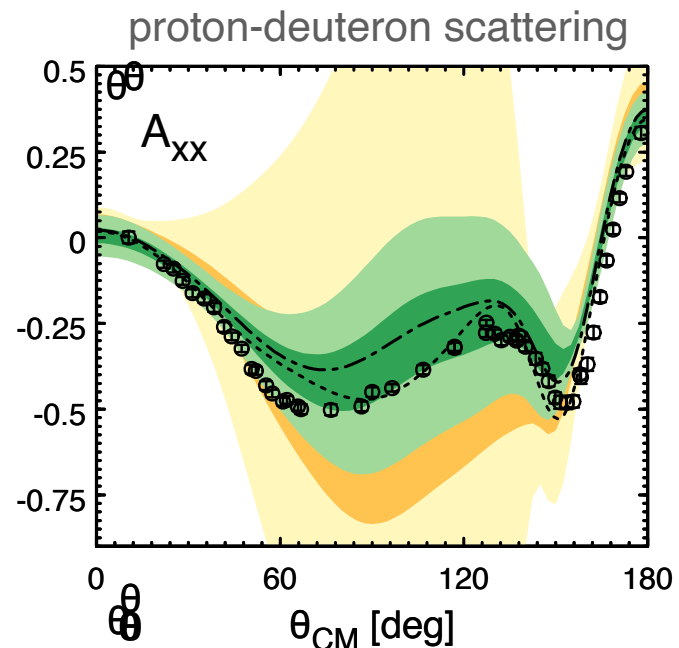
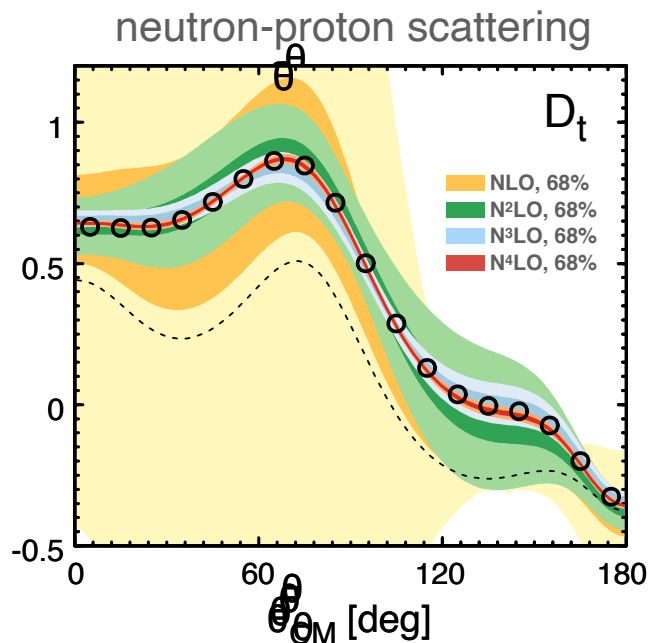
Charge radii: A smoking gun?



3. The need for a consistent regularization

Chiral EFT at N⁴LO is expected to achieve a precision sufficient for solving the 3NF problem!

So, why are we not there yet??



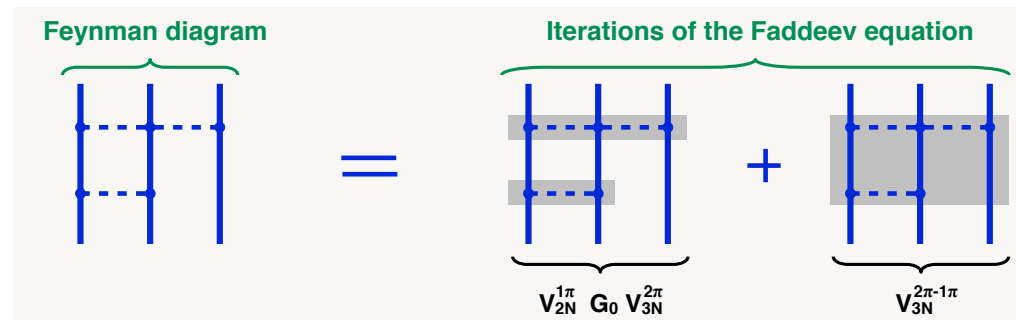
Need to address **computational** and **conceptual** challenges:

- on the computational side: determination of LECs in the 3NF ($\sim 10^7$ more CPU time needed to compute the 3N amplitude as compared to the 2N one)

3. The need for a consistent regularization

Conceptual challenge: 3NFs have been worked out using **dimensional regularization**. Is it **consistent** to employ an additional cutoff regulator when solving the Faddeev equation?

Consistency can be tested explicitly by calculating (perturbatively) the on-shell amplitude.



- Using DimReg everywhere: l.h.s. = r.h.s. \Rightarrow **consistent**
- Calculate the iterative diagram on the r.h.s. using cutoff regularization:

$$V_{2N,\Lambda}^{1\pi} G_0 V_{3N,\Lambda}^{2\pi} = -\Lambda \frac{g_A^4}{96\sqrt{2}\pi^3 F_\pi^6} \left[\underbrace{\tau_1 \cdot \tau_3 (\vec{q}_3 \cdot \vec{\sigma}_1)}_{\text{absorbable into } c_D: \text{X}} - \frac{4}{3} (\tau_2 \cdot \tau_3 - \tau_1 \cdot \tau_3) (\vec{q}_2 \cdot \vec{\sigma}_3) \right] \frac{\vec{q}_3 \cdot \vec{\sigma}_3}{q_3^2 + M_\pi^2} + \dots$$

violates chiral symmetry...

\Rightarrow all expressions for the 3NF (and exchange currents) beyond tree level, i.e. N²LO must be re-calculated using cutoff regularization that maintains chiral symmetry.

- e.g., the higher-derivative [Slavnov '71] or gradient flow regularization [Lüscher '10]
- a new path-integral approach to derive nuclear forces and currents [Krebs, EE, in preparation]

Electroweak currents

Current operators

- Switch on external sources s, p, r_μ, l_μ and consider *local* chiral rotations:

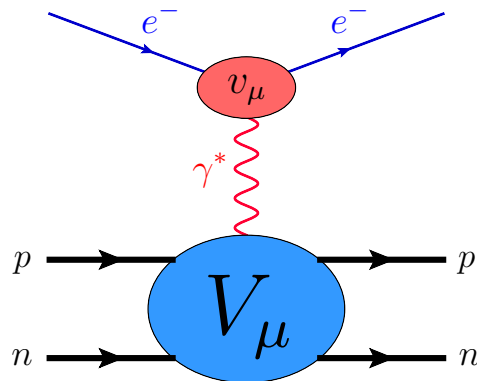
$$r_\mu \rightarrow r'_\mu = R r_\mu R^\dagger + i R \partial_\mu R^\dagger, \quad l_\mu \rightarrow l'_\mu = L l_\mu L^\dagger + i L \partial_\mu L^\dagger,$$

$$s + i p \rightarrow s' + i p' = R(s + i p) L^\dagger, \quad s - i p \rightarrow s' - i p' = L(s - i p) R^\dagger$$

- Decouple π 's to get (nonlocal) nuclear $H_{\text{eff}}[a, v, s, p]$ (MUT) & get currents via

$$V_\mu^a(\vec{x}) = \frac{\delta H_{\text{eff}}}{\delta v_\mu^a(\vec{x}, t)}, \quad A_\mu^a(\vec{x}) = \frac{\delta H_{\text{eff}}}{\delta a_\mu^a(\vec{x}, t)}$$

calculated at $a = v = p = 0, s = m_q$.

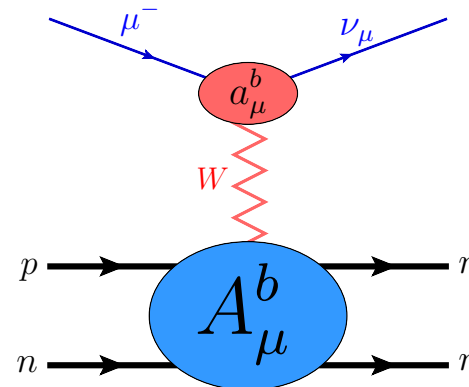


Park, Min, Rho '95

Pastore et al. (TOPT) '08 – '11: not renormalized...

Kölling, EE, Krebs, Meißner (MUT) '09,'12;

Krebs et al. '19: complete (1 loop) & renormalized



Park, Min, Rho '93

Baroni et al. (TOPT) '16: incomplete...

Krebs, EE, Meißner (MUT) '17: complete (1 loop) & renormalized,
also derived pseudoscalar currents

- about 250 topologies
- 2-loop/1-loop/tree for 1N/2N/3N operators

Also derived scalar currents, Krebs et al. '20

Continuity equations

Unexpected result: the continuity equation $\vec{k} \cdot \vec{j} \neq [H_{\text{str}}, \rho]$! Why?

Naive (MUT): $H_{\text{eff}}[h] = \underbrace{\eta U_{\text{str}}^\dagger}_{a, v, s, p} H_{\pi N}[h] U_{\text{str}} \eta$ ← cannot renormalize $V_\mu^a, A_\mu^a \dots$
 ↑ ↑ determined in the strong sector ($a = v = p = 0, s = m_q$)

Solution: employ a more general class of UT's, namely

$$H_{\text{eff}}[h, \dot{h}] = U_\eta^\dagger[h] \eta U_{\text{str}}^\dagger H_{\pi N}[h] U_{\text{str}} \underbrace{\eta U_\eta[h]}_{\text{subject to the constraint } U_\eta[0, 0, m_q, 0] = \eta} + i \left(\frac{\partial}{\partial t} U_\eta^\dagger[h] \right) U_\eta[h] \quad \leftarrow \text{induce } k_0\text{-dependence in the currents (off-shell effect...)}$$

Continuity equations = manifestations of the chiral symmetry, $h(x) \xrightarrow{\text{SU}(2)_L \times \text{SU}(2)_R} h'(x)$:
 $H_{\text{eff}}[h, \dot{h}]$ and $H_{\text{eff}}[h', \dot{h}']$ should be unitary equivalent, i.e. there exists such $U(t)$ that

$$H_{\text{eff}}[h', \dot{h}'] = U^\dagger(t) H_{\text{eff}}[h, \dot{h}] U(t) + i \left(\frac{\partial}{\partial t} U^\dagger(t) \right) U(t)$$

This implies the relations for currents $V_\mu^i(k) := \frac{\delta H_{\text{eff}}}{\delta v_\mu^i(k)}$, $A_\mu^i(k) := \frac{\delta H_{\text{eff}}}{\delta a_\mu^i(k)}$, $P^i(k) := \frac{\delta H_{\text{eff}}}{\delta p^i(k)}$:

$$\vec{k} \cdot \vec{A}^i(\vec{k}, 0) = \left[H_{\text{str}}, A_0^i(\vec{k}, 0) - \frac{\partial}{\partial k_0} \left(\vec{k} \cdot \vec{A}^i(k) + [H_{\text{str}}, A_0^i(k)] + im_q P^i(k) \right) \right] + im_q P^i(\vec{k}, 0)$$

$$\vec{k} \cdot \vec{V}^i(\vec{k}, 0) = \left[H_{\text{str}}, V_0^i(\vec{k}, 0) - \frac{\partial}{\partial k_0} \left(\vec{k} \cdot \vec{V}^i(k) + [H_{\text{str}}, V_0^i(k)] \right) \right]$$

Chiral expansion of electromagnetic currents

Kölling, EE, Krebs, Meißner, PRC 80 (09) 045502; PRC 86 (12) 047001; Krebs, EE, Meißner, arXiv:1902.06839 [nucl-th]

single-nucleon

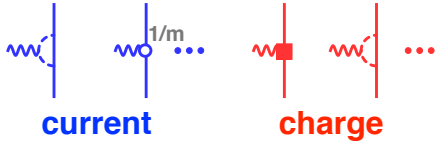
two-nucleon

three-nucleon

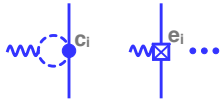
Q^{-3}



Q^{-1}



Q^0



Q^1



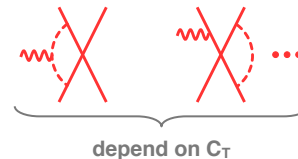
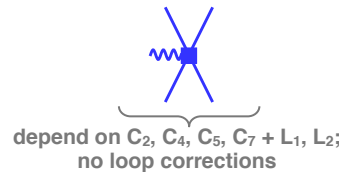
depend on $d_8, d_9, d_{18}, d_{21}, d_{22}$,
no $1/m$ corrections...

parameter-free

parameter-free



parameter-free static two-pion exchange



The expressions for em currents are off-shell consistent with the nuclear potentials derived by our group

Chiral expansion of electromagnetic currents

Kölling, EE, Krebs, Meißner, PRC 80 (09) 045502; PRC 86 (12) 047001; Krebs, EE, Meißner, arXiv:1902.06839 [nucl-th]

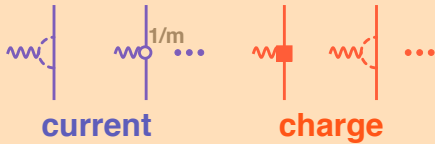
single-nucleon

two-nucleon

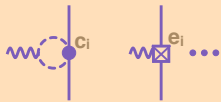
Q^{-3}



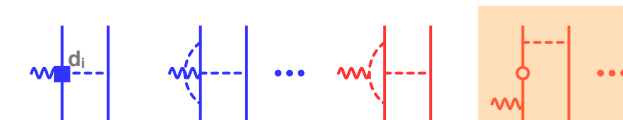
Q^{-1}



Q^0



Q^1



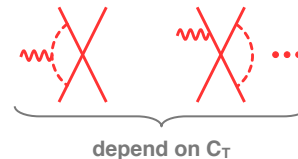
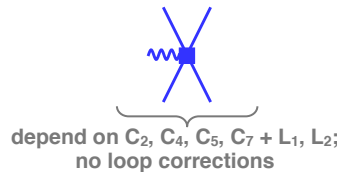
depend on $d_8, d_9, d_{18}, d_{21}, d_{22}$,
no $1/m$ corrections...

parameter-free

Can be parametrized
in terms of the
nucleon FFs



parameter-free static two-pion exchange



For review see:
H. Krebs, EPJA 56 (2020) 240

The contributions to the
exchange currents starting
from N³LO have to be
rederived using consistent
regularization...

+ N⁴LO:



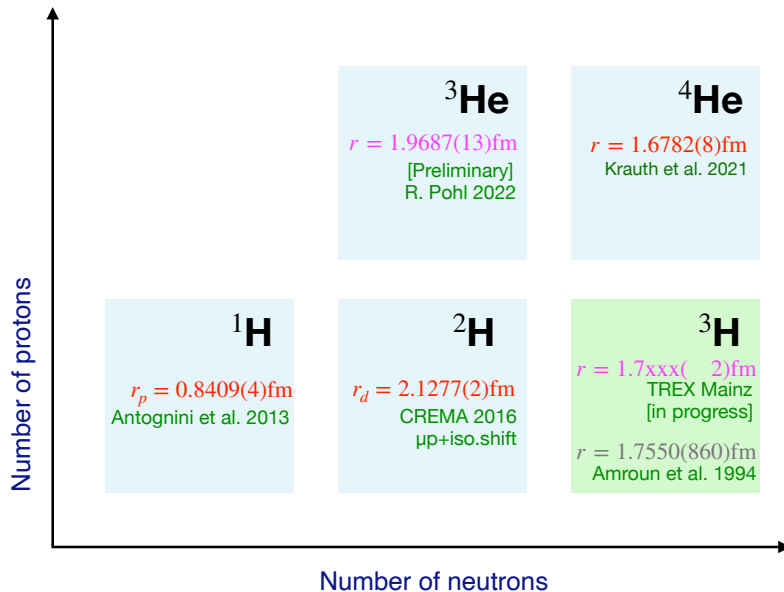
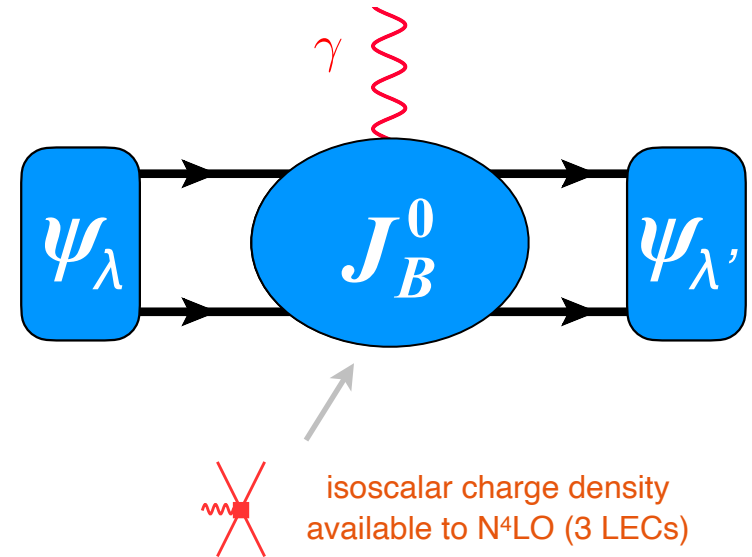
Precision determinations of charge radii of light nuclei

The charge radii are defined as a slope of the charge form factor G_C :

$$r_C^2 = (-6) \frac{\partial G_C(Q^2)}{\partial Q^2} \Big|_{Q^2=0}$$

What we calculate in the **structure radius**, which incorporates all nuclear effects:

$$r_C^2 = r_{str}^2 + \left(r_p^2 + \frac{3}{4m_p^2} \right) + \frac{A-Z}{Z} r_n^2$$



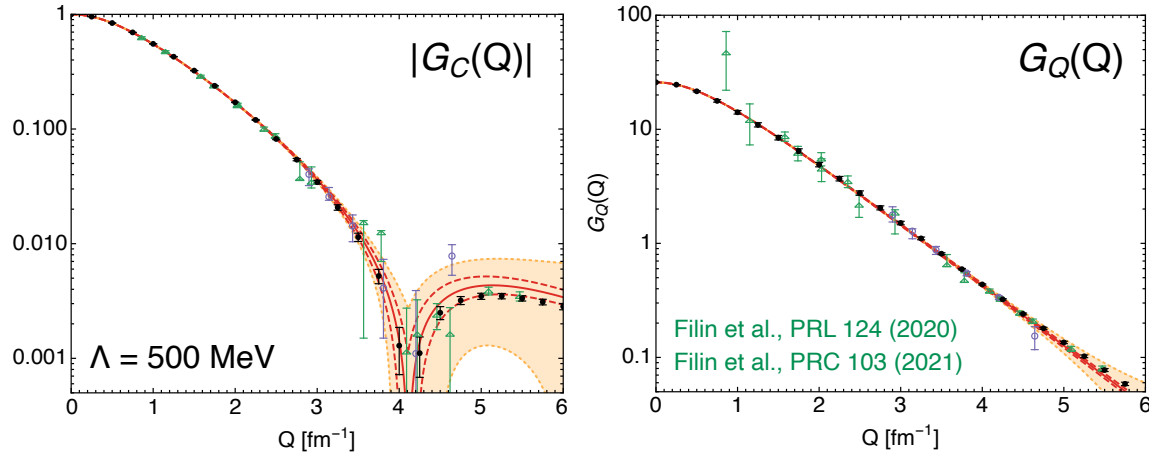
Motivation:

- precision tests of chiral EFT
- **new source of information on r_p , r_n** (provided nuclear effects under control)
- shed new light on p/d radius puzzles
- fix LECs in the short-range charge density \Rightarrow **predictions for larger A**

Deuteron charge and quadrupole FFs

Filin, Möller, Baru, EE, Krebs, Reinert, PRL 124 (2020) 082501; PRC 103 (2021) 024313

The charge and quadrupole form factors of the deuteron at N⁴LO



The extracted structure radius and quadrupole moment:

$$r_{\text{str}} = 1.9729^{+0.0015}_{-0.0012} \text{ fm}$$

$$Q_d = 0.2854^{+0.0038}_{-0.0017} \text{ fm}^2$$

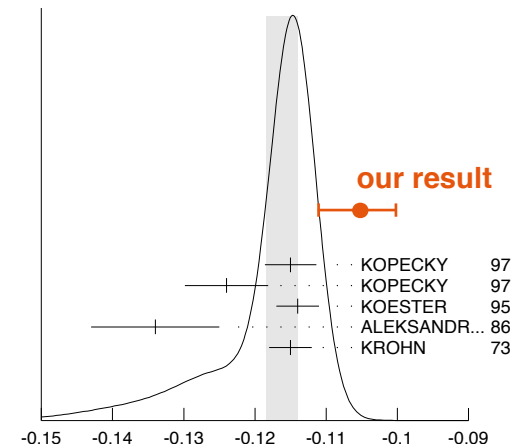
statistical and systematic errors due to the EFT truncation, choice of fitting range and π N LECs

The value of Q_d is to be compared with $Q_d^{\text{exp}} = 0.285\,699(15)(18) \text{ fm}^2$ Puchalski et al., PRL 125 (2020)

Combining our result for $r_{\text{str}}^2 = r_d^2 - r_p^2 - r_n^2 - \frac{3}{4m_p^2}$ with the

^1H - ^2H isotope shift datum $r_d^2 - r_p^2 = 3.82070(31) \text{ fm}^2$ leads to the prediction for the neutron radius:

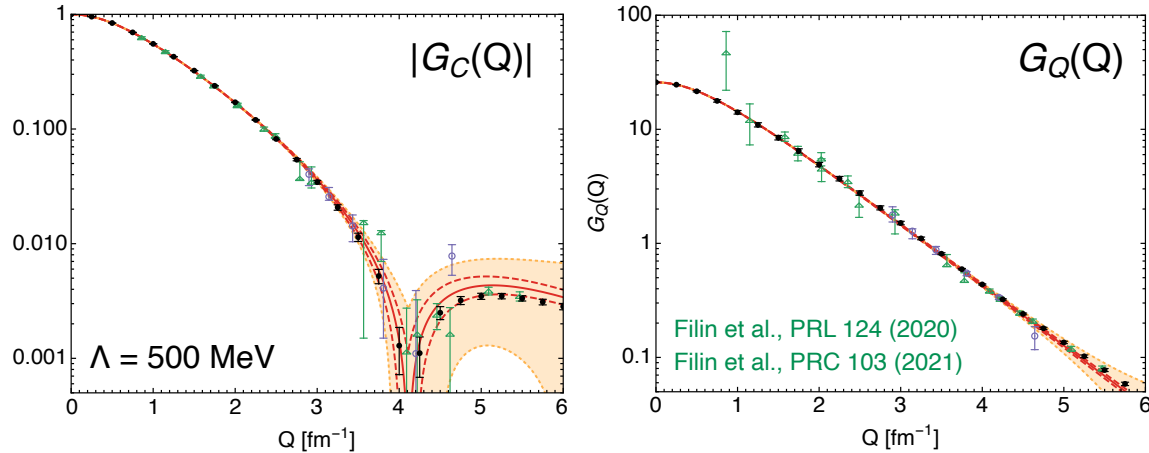
$$r_n^2 = -0.105^{+0.005}_{-0.006} \text{ fm}^2$$



Deuteron charge and quadrupole FFs

Filin, Möller, Baru, EE, Krebs, Reinert, PRL 124 (2020) 082501; PRC 103 (2021) 024313

The charge and quadrupole form factors of the deuteron at N⁴LO



The extracted structure radius and quadrupole moment:

$$r_{\text{str}} = 1.9729^{+0.0015}_{-0.0012} \text{ fm}$$

$$Q_d = 0.2854^{+0.0038}_{-0.0017} \text{ fm}^2$$

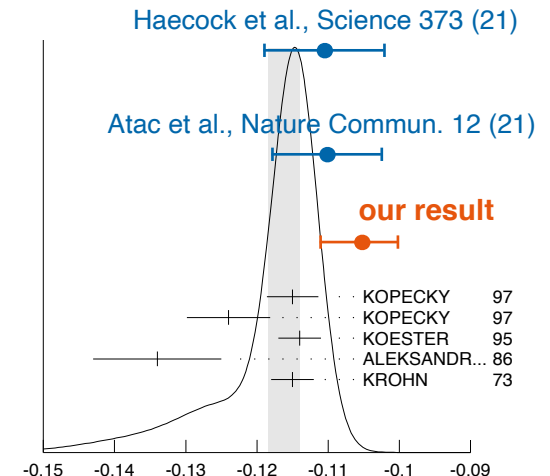
statistical and systematic errors due to the EFT truncation, choice of fitting range and π N LECs

The value of Q_d is to be compared with $Q_d^{\text{exp}} = 0.285\,699(15)(18) \text{ fm}^2$ Puchalski et al., PRL 125 (2020)

Combining our result for $r_{\text{str}}^2 = r_d^2 - r_p^2 - r_n^2 - \frac{3}{4m_p^2}$ with the

¹H-²H isotope shift datum $r_d^2 - r_p^2 = 3.82070(31) \text{ fm}^2$ leads to the prediction for the neutron radius:

$$r_n^2 = -0.105^{+0.005}_{-0.006} \text{ fm}^2$$



Charge radii of light nuclei

Filin, Baru, EE, Körber, Krebs, Möller, Nogga, Reinert, in preparation

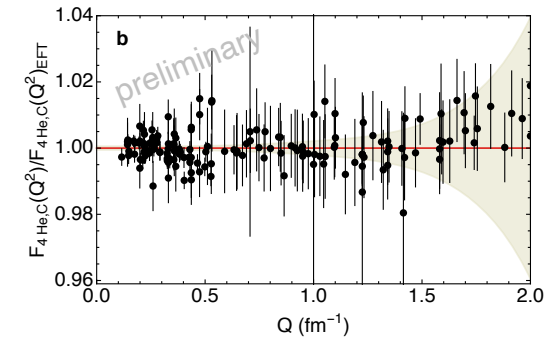
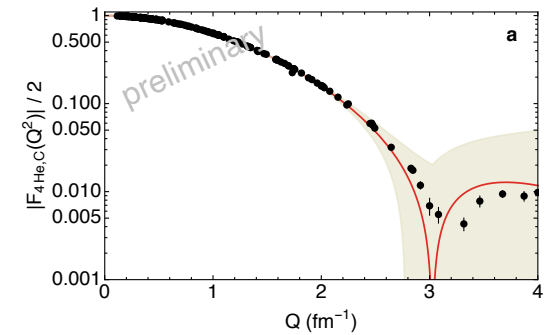
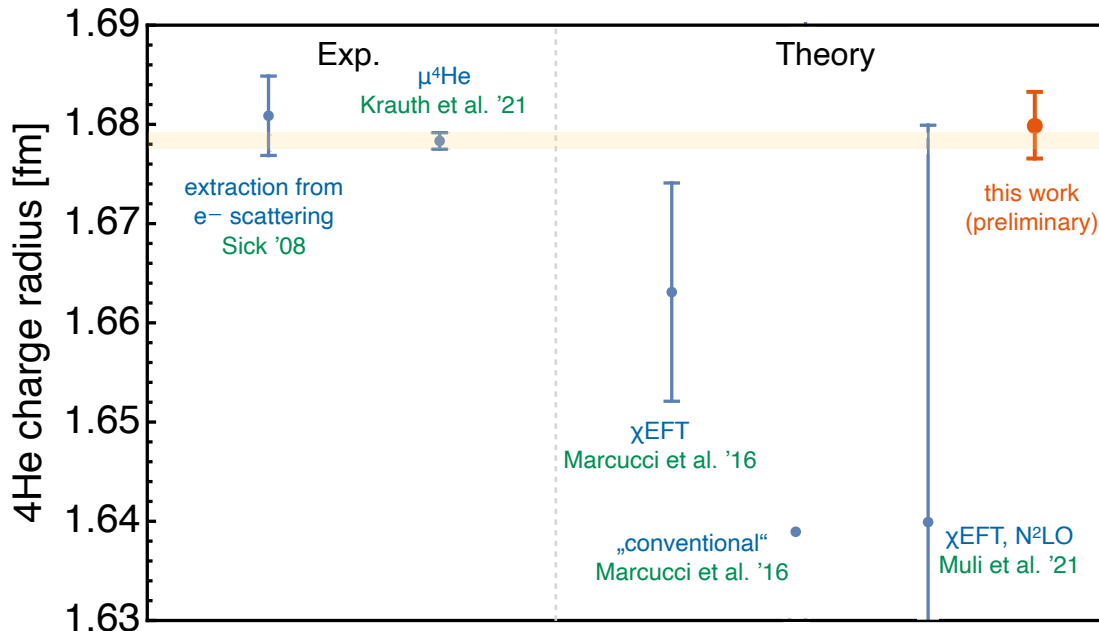
2 out of 3 LECs in the short-range 2N charge density already fixed from the ^2H FFs; the remaining one is determined from the ^4He FF (lots of low-energy data...)

$$r_{str}(^4\text{He}) = 1.4784 \pm 0.0030_{\text{trunc}} \pm 0.0013_{\text{stat}} \pm 0.0007_{\text{num}} \text{ fm}$$

preliminary; relativistic corrections still under investigation

$$\Rightarrow r_C(^4\text{He}) = 1.6798 \pm 0.0035 \text{ fm}$$

using CODATA r_p and own determination of r_n



The μ 4He exp. value is:

$$r_C^{\text{exp}}(^4\text{He}) = (1.67824 \pm 0.00083) \text{ fm}$$

Krauth et al., Nature 589 (2021) 7843, 527-531

Charge radii of light nuclei

Filin, Baru, EE, Körber, Krebs, Möller, Nogga, Reinert, in preparation

With all LECs being fixed, we can predict the isoscalar 3N charge radius $\sqrt{\frac{1}{3}r_C^2(^3\text{H}) + \frac{2}{3}r_C^2(^3\text{He})}$

$$r_C(3N_{\text{isoscalar}}) = (1.9058 \pm 0.0026) \text{ fm}$$

preliminary, using CODATA-2018 r_p and own determination of r_n

On the experimental side:

— the ^3H radius poorly known (5%) from e^- scattering exp.: $r_C^{^3\text{H}} = (1.755 \pm 0.086) \text{ fm}$
Amroun et al. '94 (world average)

— more (and more precise) measurements for ^3He

— e^- scattering experiments: $r_C^{^3\text{He}} = (1.973 \pm 0.016) \text{ fm}$ Sick '15 (world average)

— muonic ^3He (preliminary): $r_C^{^3\text{He}} = (1.9687 \pm 0.0013) \text{ fm}$ Pohl '22

⇒ the current exp. value for the isoscalar radius: $r_C^{\text{exp}}(3N_{\text{isoscalar}}) = (1.903 \pm 0.029) \text{ fm}$

The ongoing T-REX experiment in Mainz [Pohl et al.] aims at measuring $r_C^{^3\text{H}}$ with $\pm 0.0002 \text{ fm}$, which would determine the isoscalar radius with $\pm 0.0009 \text{ fm}$ ⇒ precision tests of nuclear chiral EFT!

MEC contribution increases from $\sim 0.3\%$ for ^2H to $\sim 3\%$ for ^4He !

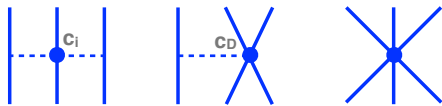
Axial currents

Krebs, EE, Meißner, Annals Phys. 378 (2017) 317

Chiral expansion of the axial **current** and **charge** operators

	single-nucleon	two-nucleon	three-nucleon
Q^{-3}			
Q^{-1}			
Q^0			
Q^1			

Pion-pole contributions are directly related to the corresponding topologies in the nuclear forces. E.g., the leading 3NF:



Chiral EFT and lattice QCD

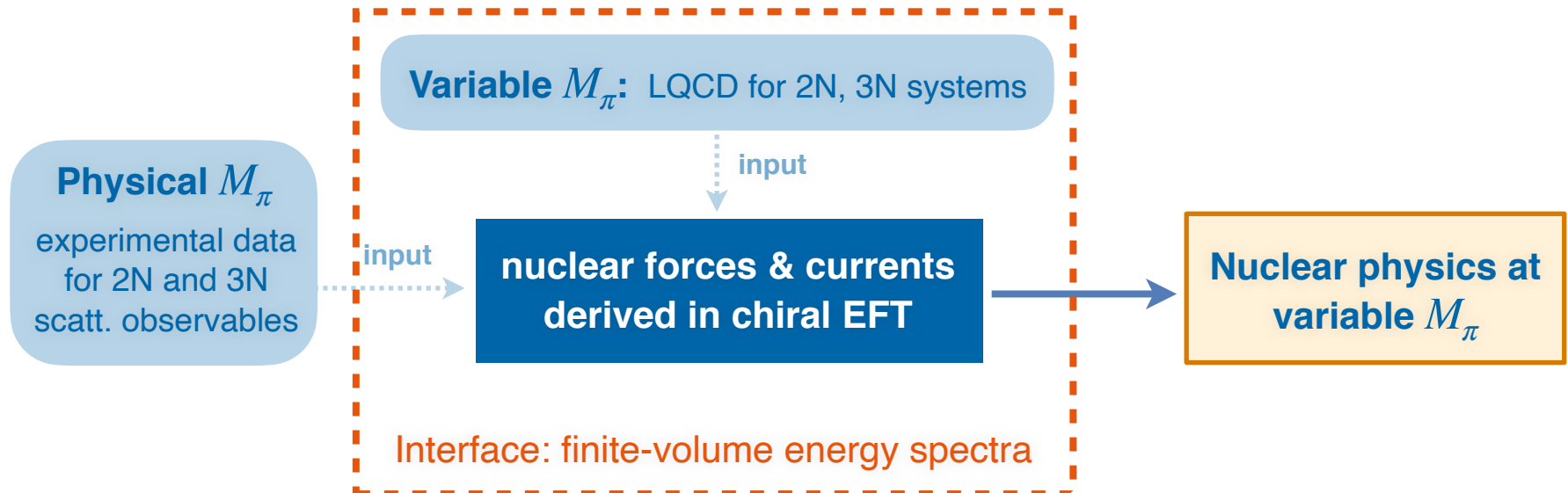
Introduction

Variable M_π : no experimental data available \Rightarrow need LQCD input

EFT as a tool to extrapolate LQCD results for few-N systems:

- chiral extrapolations Beane, Savage, EE, Meißner, Soto, Bedaque, Lee, Lähde, Long, Gegelia, ...
 - in E beyond the t -channel cut at fixed M_π (low-energy theorems) EE, Baru, Filin, Gegelia
 - in the number of nucleons at fixed M_π (so far π -less EFT) Barnea, Bazak, van Kolck, Detmold, ...
- Closer to the physical point, pions are to be included as explicit DoF \Rightarrow **chiral EFT**

Long-term goal:



Two nucleons in a finite box (spin-0 channels)

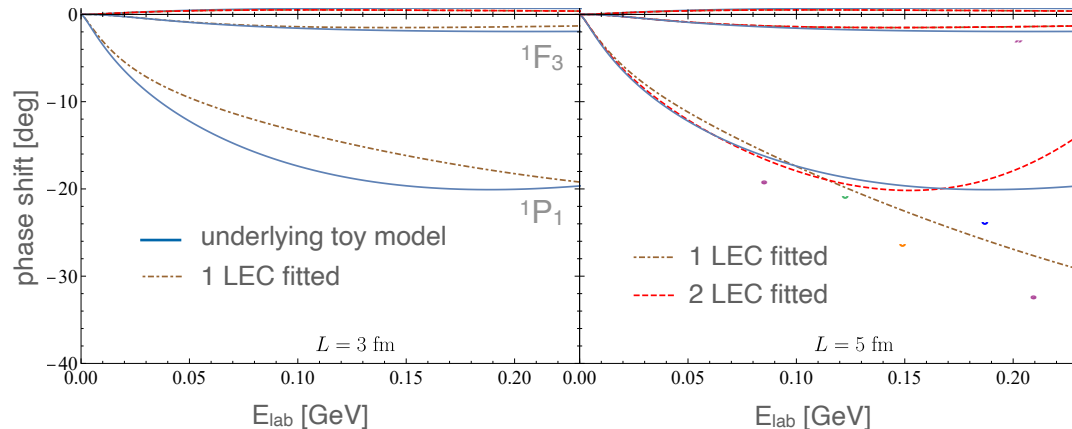
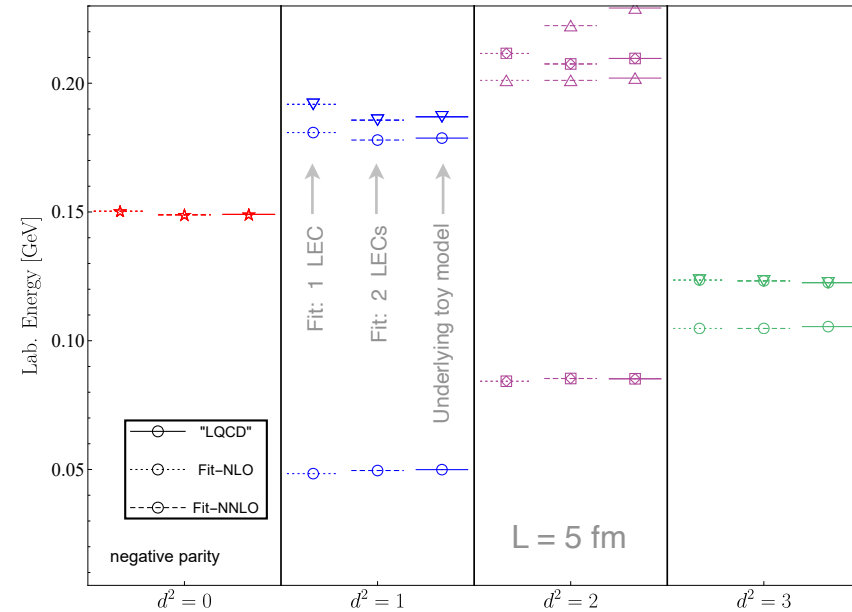
Lu Meng, EE, JHEP 10 (2021) 051

2-body phase shifts can be extracted from finite-volume energy spectra using Lüscher's formula.

For NN scattering near the physical pion mass, **1-channel Lüscher formula is expected to break down due to partial wave mixing** (π -exchange, especially neg. parity states)

Proposed alternative:

- use χ EFT to describe the long-range interactions and to parametrize the short-range ones
- calculate finite-volume energy in the plane-wave basis (no reliance on the PW expansion)
- fit LECs to finite-volume energies and determine phase shifts in the continuum



Toy-model example

$$V_{\text{toy}} = - \underbrace{\left(\frac{g_A}{2F_\pi} \right)^2 \frac{M_\pi^2}{q^2 + M_\pi^2} \boldsymbol{\tau}_1 \cdot \boldsymbol{\tau}_2}_{\text{long-range}} + \underbrace{(c_{h1} + c_{h2} \boldsymbol{\tau}_1 \cdot \boldsymbol{\tau}_2) \frac{1}{q^2 + m_h^2}}_{\text{short-range}}$$

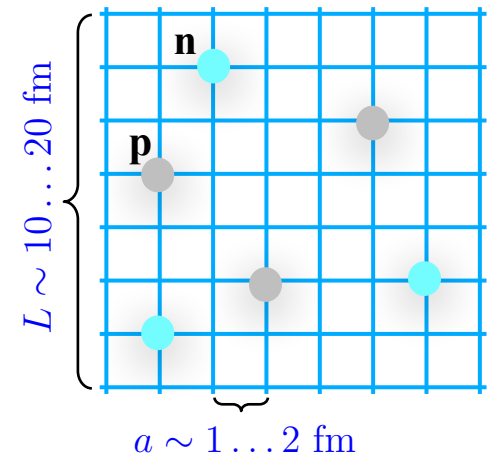
$$V_{\text{EFT}} = - \left(\frac{g_A}{2F_\pi} \right)^2 \frac{M_\pi^2}{q^2 + M_\pi^2} \boldsymbol{\tau}_1 \cdot \boldsymbol{\tau}_2 + V_{\text{cont}}^{(0)} + V_{\text{cont}}^{(2)} + V_{\text{cont}}^{(4)} + \dots$$

Nuclear lattice simulations

D. Lee, U.-G. Meißner, J. Drut, S. Elhatisari, EE, H. Krebs, T. Lähde, B-N. Lu, T. Luu, G. Rupak + post-docs + students

— more than 40 publications including many PRL and 1 Nature —

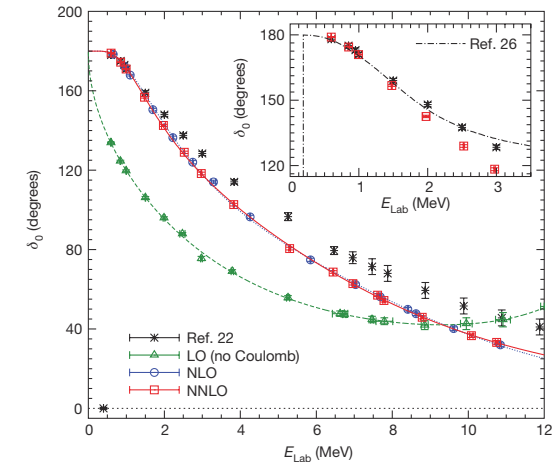
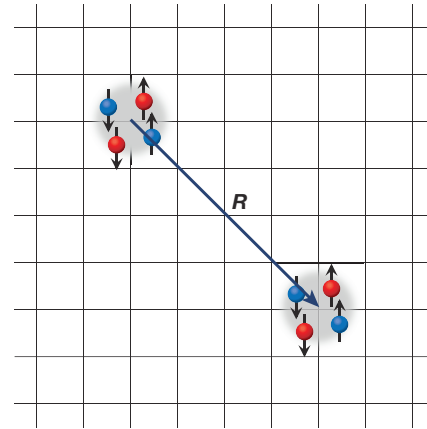
- A discretized, Euclidean-time formulation of chiral EFT
- Access to nuclei via Auxiliary Field Quantum Monte Carlo simulations
- Nuclear clustering automatically taken into account
 - Severe sign problem (unless the action is SU(4) invariant)
 - The strategy: start with the nearly SU(4) invariant LO action and include corrections in perturbation theory



Nuclear lattice simulations

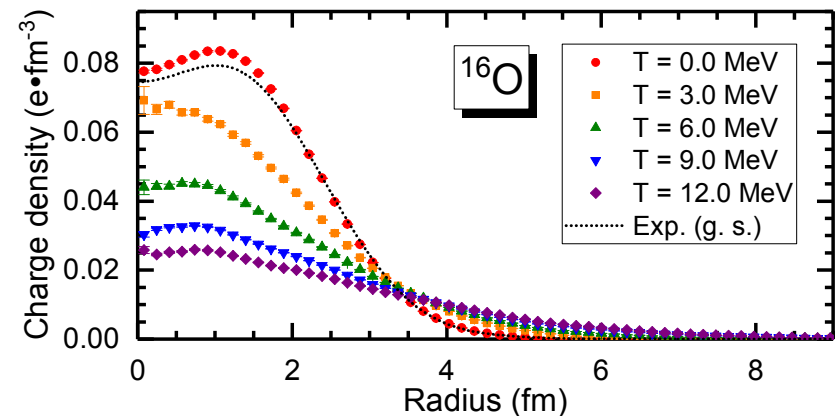


Used lattice EFT to extract the effective Hamiltonian for two interacting α -clusters (the adiabatic projection method)



Some recent developments and highlights

- Demonstrated that only 4 (!) parameters (S-wave scattering length and range in the SU(4) limit, strength of the 3NF and strength of the local NN force) are sufficient to accurately describe main nuclear properties [Bing-Nan Lu et al., PLB 797 \(2019\) 134863](#)
- Introduced the pinhole algorithm to perform **ab initio simulations at finite temperature** [Bing-Nan Lu et al., PRL 125 \(2020\) 192502](#)
- Explored the relationship between the approx. Wigner and spin-isospin exchange symmetries [Dean Lee et al., PRL 127 \(2021\) 062501](#)



Summary Day 5

- The NN sector of chiral EFT is in a good shape: **a perfect description of np and pp data at N⁴LO⁺**. Good convergence of χ -expansion for forces! Extraction of the π N couplings from np and pp data is in progress.
- Deuteron charge and quadrupole FFs: **accurate results at low q; nuclear effects well under control**. Preliminary results for the charge radii of A=3 and A=4 systems look promising. **Role of ρ_{2N} in heavier-mass nuclei?**
- Nuclear forces at **unphysical** quark masses: situation unclear, waiting for lattice QCD results... Established machinery for matching in finite-V.
- Nuclear lattice simulations: a novel *ab-initio* approach to nuclei **capable of describing strongly clustered states**.

(Near) future:

- Consistently regularized 3NF & currents beyond N²LO
 - PWA of 3N scattering at N⁴LO
- ⇒ open the way for precision nuclear theory

Thank you for your attention!